TECHNICAL REPORT

ISO/TR 9705-2

First edition
2001-05-01

Reaction-to-fire tests — Full-scale room tests for surface products —

Part 2:
Technical background and guidance

Essais de réaction au feu — Essais dans une pièce en vraie grandeur pour les matériaux de revêtement intérieur —

Partie 2: Données techniques et lignes directrices

© ISO 2001

Contents

Page

© ISO 2001 — All rights reserved

Foreword

ISO (the International Organization for Standardization) is a worldwide federation of national standards bodies (ISO member bodies). The work of preparing International Standards is normally carried out through ISO technical committees. Each member body interested in a subject for which a technical committee has been established has the right to be represented on that committee. International organizations, governmental and non-governmental, in liaison with ISO, also take part in the work. ISO collaborates closely with the International Electrotechnical Commission (IEC) on all matters of electrotechnical standardization.

International Standards are drafted in accordance with the rules given in the ISO/IEC Directives, Part 3.

The main task of technical committees is to prepare International Standards. Draft International Standards adopted by the technical committees are circulated to the member bodies for voting. Publication as an International Standard requires approval by at least 75 % of the member bodies casting a vote.

In exceptional circumstances, when a technical committee has collected data of a different kind from that which is normally published as an International Standard ("state of the art", for example), it may decide by a simple majority vote of its participating members to publish a Technical Report. A Technical Report is entirely informative in nature and does not have to be reviewed until the data it provides are considered to be no longer valid or useful.

Attention is drawn to the possibility that some of the elements of this part of ISO/TR 9705 may be the subject of patent rights. ISO shall not be held responsible for identifying any or all such patent rights.

ISO/TR 9705-2 was prepared by Technical Committee ISO/TC 92, *Fire safety*, Subcommittee SC 1, *Fire initiation and growth*.

ISO 9705 consists of the following parts, under the general title *Reaction-to-fire tests — Full-scale room tests for surface products*:

⎯ *Part 1: Full-scale test for surface products* (currently published as ISO 9705:1993*, Fire tests — Full-scale room test for surface products*)

⎯ *Part 2: Technical background and guidance* [Technical Report]

Introduction

ISO 9705:1993 specifies a test method simulating a fire that starts under well-ventilated conditions, in a corner of a small room with a single open doorway.

The method is intended to evaluate the contribution to fire growth provided by a surface product using a specified ignition source. The method provides data for a specified ignition source for the early stages of a fire from ignition up to flashover. ISO 9705:1993 also describes different measurement techniques inside and outside the room. This part of ISO 9705 gives background information and support to the potential users of the test. It gives the user of the test technical information on the ignition source, heat fluxes in the room from the burner, heat balance in the room during a fire, aspects of smoke production and toxic gas species production, as well as aspects of modelling the results of these tests. It gives the user the information necessary to select the testing procedure for specific projects or regulations.

Reaction-to-fire tests — Full-scale room tests for surface products —

Part 2:
Technical background and guidance

1 Scope

This part of ISO 9705 provides guidance on ISO 9705:1993. It describes the technical background of the test and gives information which may be used for determining a testing procedure for a specific scenario, or how results can be utilized in a total hazard analysis for the specified scenario.

2 Characteristics of the ignition sources

2.1 Standard ignition source

The standard ignition source consists of a sandbox burner with dimensions of 0,17 m × 0,17 m. This source is used in reference [1] (see Bibliography). An important characteristic of the ignition source is its heat transfer towards the material. Figures 1 and 2 show a detailed mapped overview of the total heat flux towards the specimen and the gas temperatures. The measurements are performed in an open wall configuration, at an energy release rate level of 100 kW [2]. These values will slightly change when the burner is located in a room environment. Figures 3 and 4 give the contours of a constant heat flux of 10 kW/m^2 at different heat outputs of the burner and also where areas of total heat flux are higher than a given value.

2.2 Alternative ignition source

One of the alternative heat sources is a box burner, with dimensions of 0,3 m × 0,3 m. It is described in ASTM E603-98 [3]. Figures 5 and 6 give a detailed mapping of heat fluxes and gas temperatures for a burner energy release rate of 160 kW [2]. Other heat sources may be more appropriate (see annex B of ISO 9705:1993). Figure 7 gives results of heat fluxes towards the specimen for a heat source level of 40 kW and 160 kW, with different gases (natural gases and a mixture of natural gas and toluene) [4]. Figures 8 and 9 show a comparison of different burner sizes for contours of constant heat flux of 10 kW/m^2, at an energy release rate of 100 kW in an open corner and for areas exposed to a certain irradiant heat flux [4].

Finally, an example is given of the difference between the total heat flux produced by a burner in a corner and a wall position. Table 1 gives an overview of the total heat flux towards the floor and the total heat flux to the wall at 0,9 m and 1,5 m height for energy release rates of 40 kW and 160 kW using the alternative ignition source of ISO 9705:1993. Results show that, for the corner position, heat flux levels are higher in almost all cases.
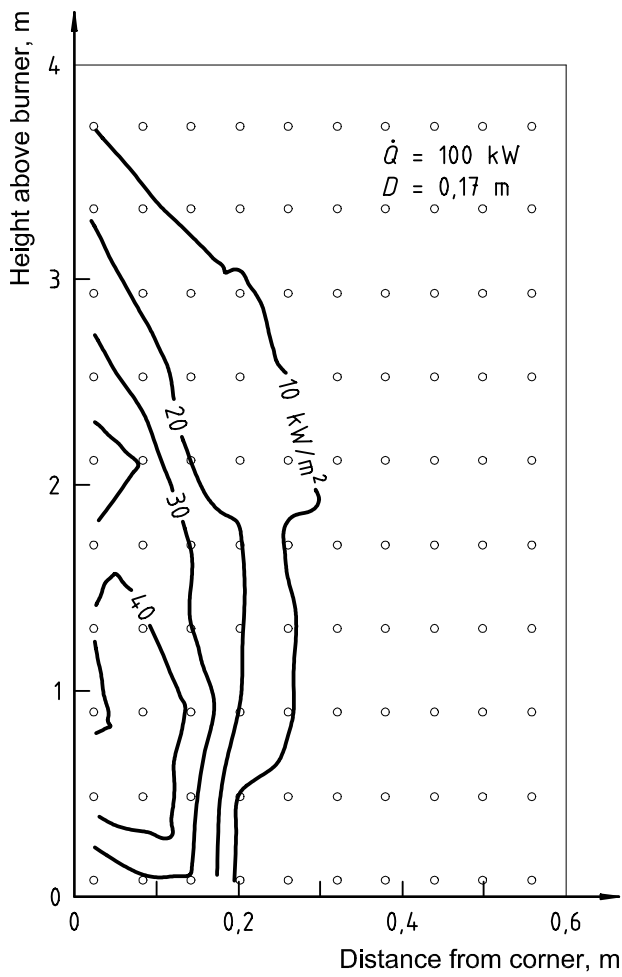
Figure 1 — Heat flux distribution at an energy release rate of 100 kW for the standard ignition source in an open corner
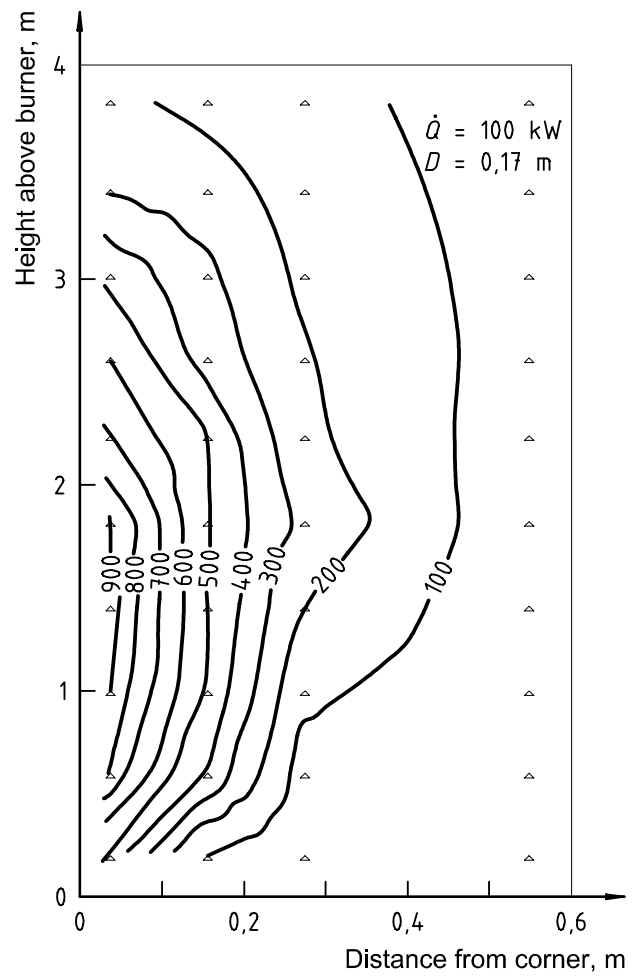
Figure 2 — Gas temperature distribution 30 mm from the wall at an energy release rate of 100 kW for the standard ignition source in an open corner
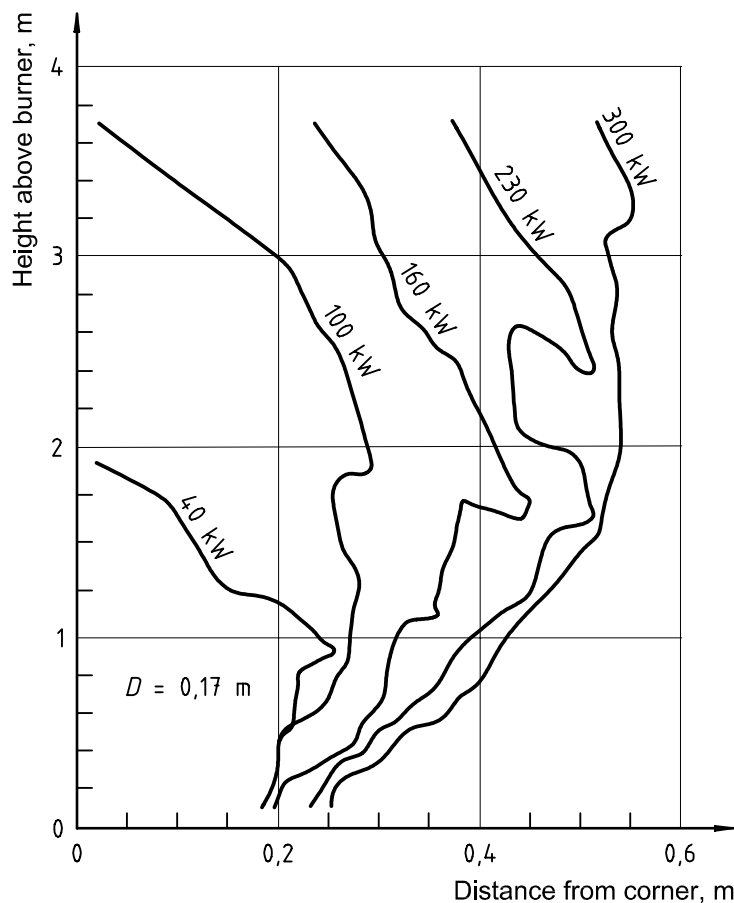
NOTE   Contours of 10 kW/m^2.

Figure 3 — Contours of constant heat flux for the standard ignition source in an open corner at different irradiant heat flux levels
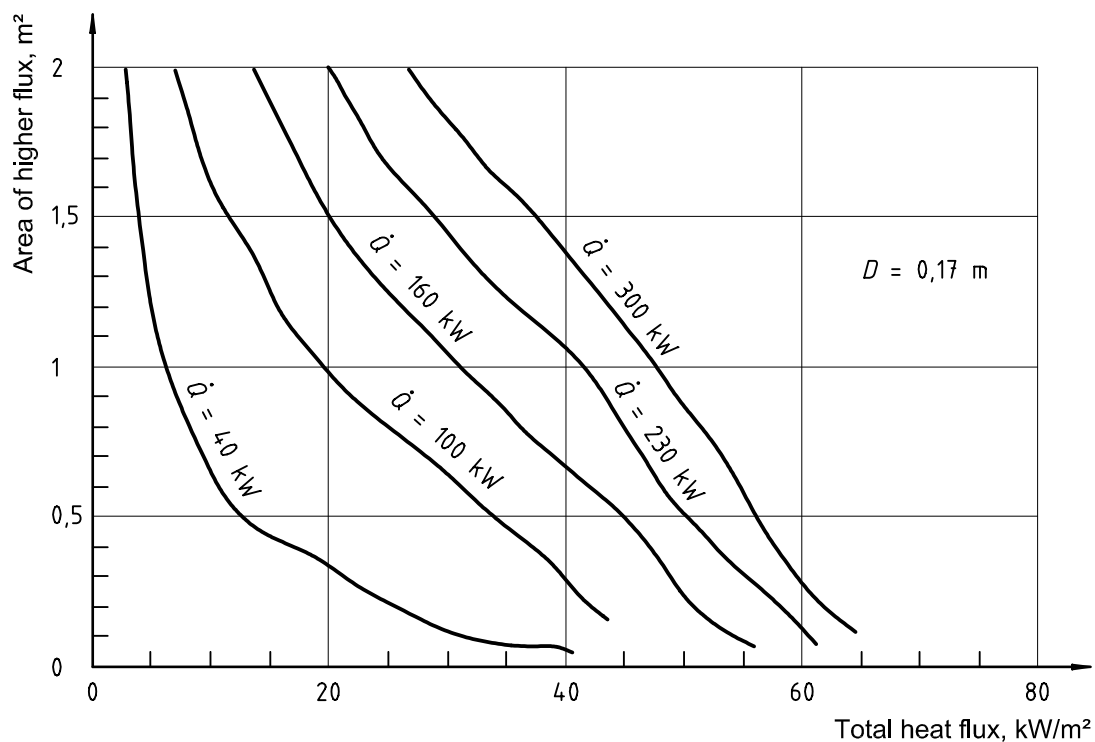
Figure 4 — Areas of total heat flux levels higher than a given value for the standard ignition source at different irradiant heat flux levels in an open corner

© ISO 2001 – All rights reserved
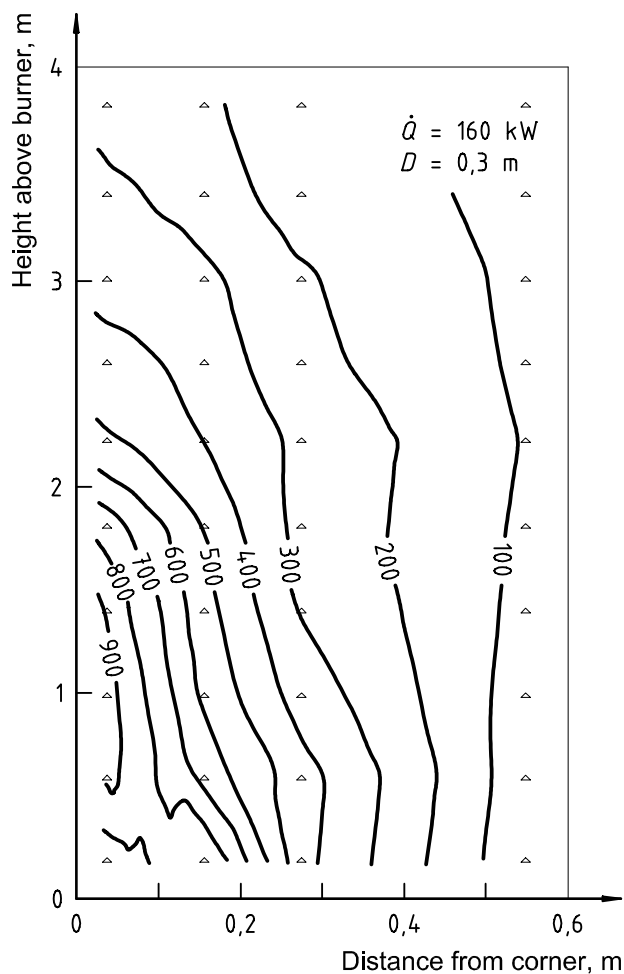
Figure 5 — Heat flux distribution at 160 kW for the alternative ignition source in an open corner
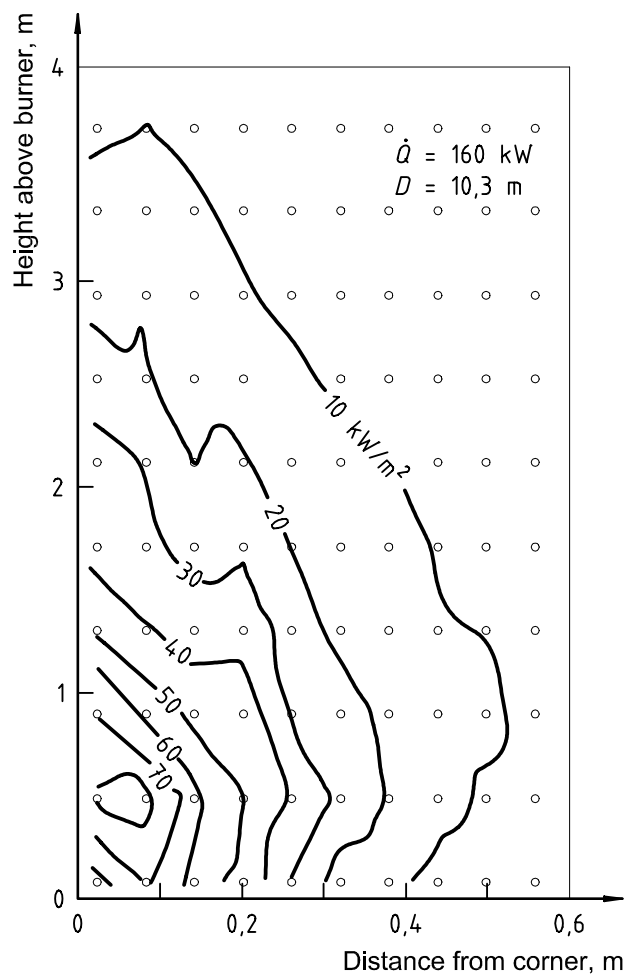
Figure 6 — Gas temperature distribution 30 mm from the wall at 160 kW for the alternative ignition source in an open corner
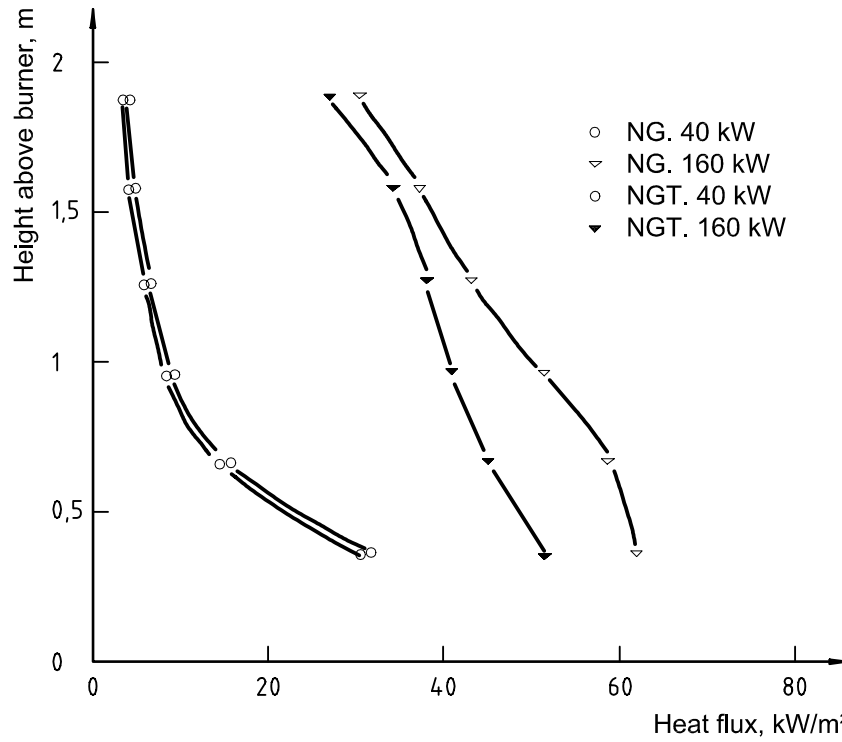
Figure 7 — Heat flux distribution for the alternative ignition source in an open corner at 40 kW and 160 kW with different types of gas
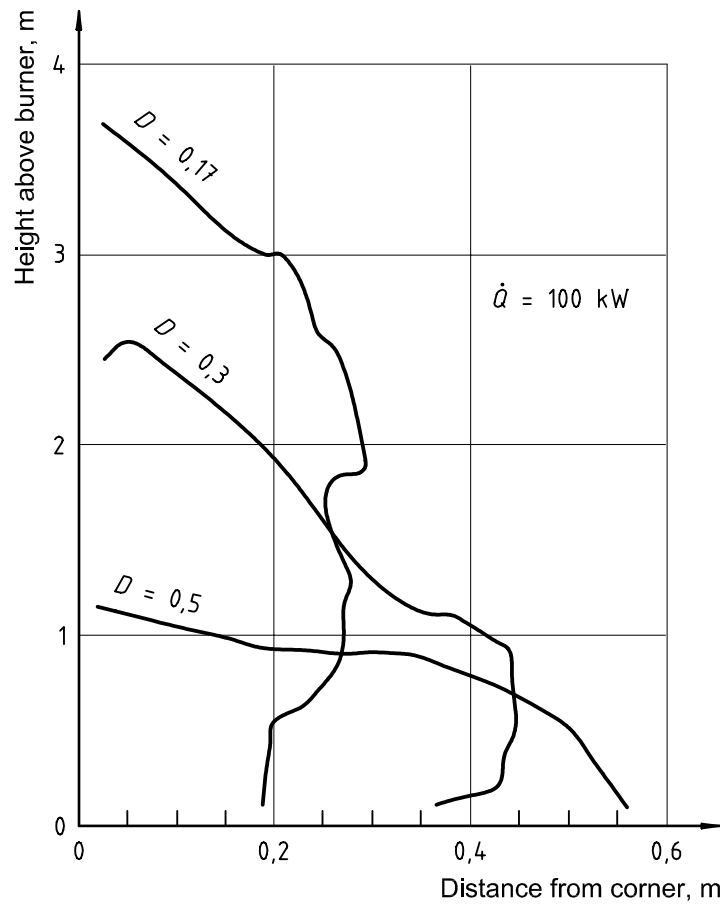
NOTE   Contours of 10 kW/m².

Figure 8 — Contours of constant heat flux for the different sizes of box ignition sources in an open corner at a 100 kW heat source level

© ISO 2001 — All rights reserved

Not for Resale
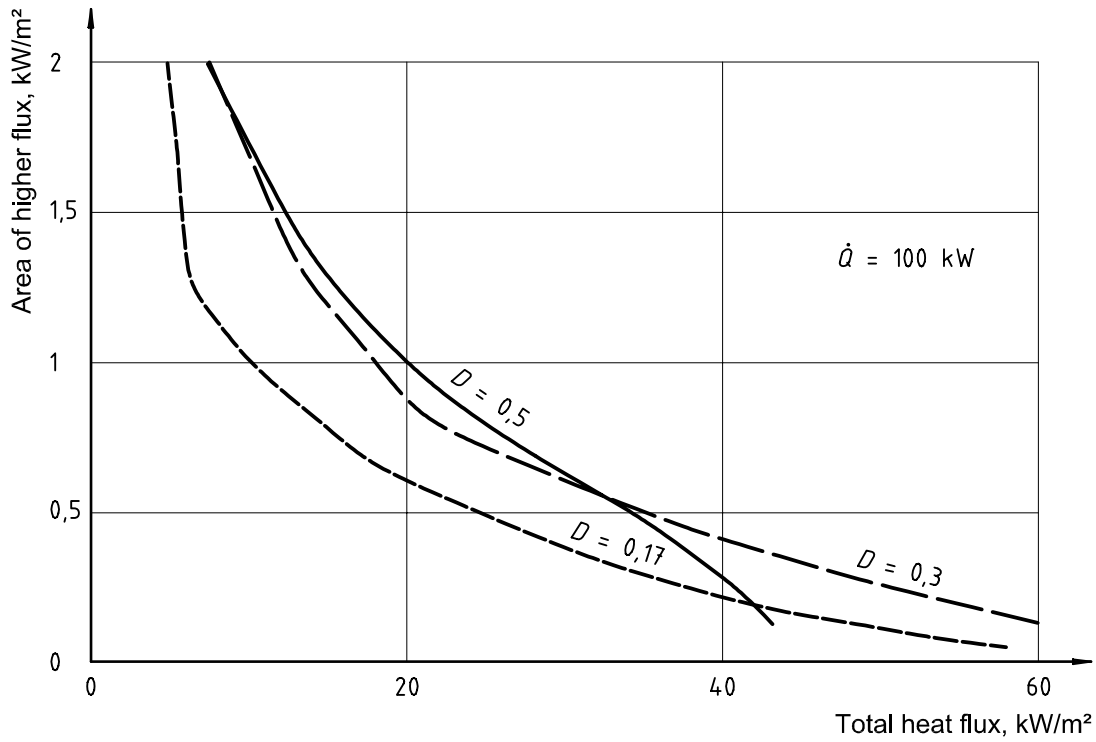
Figure 9 — Areas of total heat flux levels higher than a given value for different box ignition sources at 100 kW in an open corner

Table 1 — Comparison between corner and centre wall position

Heat source level	Burner in the corner			Burner at centre of back wall		
	Heat flux to floor kW/m^2	Heat flux to wall at 0,9 m kW/m^2	Heat flux to wall at 1,5 m kW/m^2	Heat flux to floor kW/m^2	Heat flux to wall at 0,9 m kW/m^2	Heat flux to wall at 1,5 m kW/m^2
40 kW	0,6	12,5	6,5	0,6	8,5	4
160 kW	5,4	56	60	4,2	62	33

3 Sensitivity analyses

3.1 General

Various sensitivity analyses have been performed over the last 25 years. All studies used the room described in ISO 9705:1993, but differed in the type of ignition source (the standard ignition source or the alternative ignition source of ISO 9705). These sensitivity analyses contained different specimen configurations and different ignition positions and levels. An overview is given below of some of the findings as guidance for testing in the ISO 9705 room.

3.2 Specimen configurations

Sensitivity analyses revealed that testing with linings on both ceiling and walls resulted in a more severe condition than tests with linings on the walls only [5]. When only the walls are covered with linings, a ceiling lined with ceramic wool is more severe than a ceiling lined with gypsum boards and will show less discrimination between the different materials [6].

In order to achieve comparable tests data between laboratories and high discrimination, it is recommended in ISO 9705 that the walls (excluding the wall containing the doorway) and the ceiling are covered with the product. When other specimen configurations are used, this should be clearly stated in the report.

3.3 Effect of the burner size

The effect of the burner size has been studied extensively within the Eurefic programme [7]. Results have been shown for heat flux distribution and gas temperatures. Moreover, tests were done in a room lined with particle board. Little effect was seen on the time to flashover at rates of heat release of 160 kW and 300 kW. At a lower heat release of about 40 kW, the time to flashover with a large burner (0,5 m by 0,5 m) was significantly longer than for the other burners (standard and alternative ignition source of ISO 9705). The reason for this was explained by the smaller area which is exposed to a given heat flux level (see Figure 9), hence producing a slower flame spread.

3.4 Effect of the stand-off distance of the burner

Experiments at lower heat source levels with the alternative ignition source of ISO 9705 showed that there was a considerable influence of the stand-off distance of the burner [8]. With the standard ignition source, the stand-off distance seems to be less critical. The influence can in most cases be predicted by heat flux measurements at the walls behind the burner flame.

4 Heat balance in the room

4.1 General

An energy balance calculation was carried out at the early stages on the development of the ISO 9705 room corner test [9]. The energy balance in the room can be given as follows:

$$\dot{Q}_c = \dot{Q}_{co} + \dot{Q}_w + \dot{Q}_r + \dot{Q}_b$$

where

$\dot{Q}_c$ is the heat released by combustion (kW);

$\dot{Q}_{co}$ is the heat loss by convection through the doorway (kW);

$\dot{Q}_w$ is the heat loss by conduction into the surrounding structure (kW);

$\dot{Q}_r$ is the heat loss by radiation throughout the doorway (kW);

$\dot{Q}_b$ is the heat stored in the gas volume (kW).

In most cases the heat stored in the gas volume is negligible. The other terms are calculated as given in the following paragraphs. The results of a heat balance calculation are also given below.

4.2 Heat release by combustion

Heat release by combustion might be the heat release measurement or, in the case of the calibration test, this can be calculated as

$$\dot{Q}_c = \Delta H_c \cdot \dot{m}_f$$

where

ΔH_c is the heat of combustion, equal to the net calorific value of propane (46,4 MJ/kg);

$\dot{m}_f$ is the mass loss rate of the propane (kg/s).

4.3   Heat loss by convection

The heat loss at the doorway can be calculated as follows:

$$\dot{Q}_{co} = \dot{m}_o \cdot c_p (T_g - T_a)$$

where

$\dot{m}_o$ is the mass flow rate out of the doorway (kg/s);

c_p is the specific heat of the smoke gases (kJ/kg·K);

T_g is the smoke gas temperature (K);

T_a is the ambient temperature (K).

4.4   Heat loss by conduction

The heat loss by conduction through the walls can be calculated as follows:

$$\dot{Q}_w'' = -k \left(\frac{dT}{dx} \right)_{x=0}$$

where

$\dot{Q}_w''$ is the heat conduction per unit area (W/m²);

k is the thermal conductivity (W/m·K);

$\left(\dfrac{dT}{dx} \right)_{x=0}$ is the temperature gradient at the surface (K/m).

The temperature gradient can be calculated by means of temperature measurements in and on the walls. The heat loss through the walls can also be calculated using numerical heat transfer methods.

4.5   Heat loss by radiation

The heat loss by radiation out of the doorway can be calculated by adding the contribution from a number of smaller areas from the walls and ceiling of the room:

$$\dot{Q}_r = \sigma \sum_i \varepsilon_i \cdot A_i \cdot F_i \cdot \bar{T}_i^{\,4}$$

where

σ is the Stefan Boltzmann constant ($5{,}67 \times 10^{-8}$ W/m$^2 \cdot$K^4);

ε_i is the emissivity;

A_i is the temperature gradient at the surface (K/m);

F_i is the view factor;

$\overline{T}_i$ is the absolute temperature (K).

4.6   Results of heat balance calculations

The heat balance calculations of a room test with a propane burner as heat source are given in Table 2 at steady-state conditions.

Table 2 — Results of heat balance calculations

Heat release by combustion	Heat loss by convection	Heat loss by conduction	Heat loss by radiation	Total heat loss	Difference
kW	kW	kW	kW	kW	%
125	105	19	6	129	3
250	208	32	12	252	1

5   Measuring techniques

5.1   Mass flow through the doorway and interface height

One of the methods referred to in ISO 9705 to calculate the mass flow out of the door is by means of bi-directional probes and suction pyrometers in the door opening. In many cases this is an extensive and expensive method. In the next clause some calculation methods will be given for determination of the interface height and the mass flow through the door opening. A possible set-up of instrumentation for such calculations is given in Figure 10 [6]. It should be noted that in some cases small pressures are to be measured which can influence the accuracy of the measurement.

Key
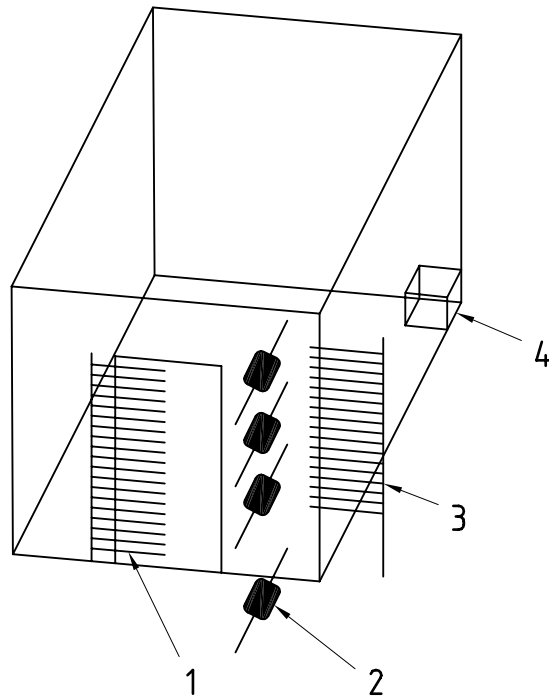
1   Door TC tree
2   Δp transducer
3   Corner TC tree
4   Corner burner

Figure 10 — Experimental set-up for different calculation methods of the interface height and mass flow rates at the door opening of the ISO 9705 room

5.2   Measurement of toxic gases

Additional to the measurement techniques given ISO 9705, techniques such as FTIR and ion chromatography have recently been applied successfully in full-scale tests. A practical example how this can be performed is given in annex B. The reader is also referred to the documents developed within ISO/TC 92/SC 3 for a complete overview of the measurement of toxic gases in combustion gases produced in fire tests.

5.3   Mass loss rate from the sample

Direct mass loss measurements of the linings can be performed by means of putting the complete room on load cells or by putting the structure on which the linings are fixed on load cells. Due to the high tare value obtained by the weight of the room, it should be noted that only limited accuracy can be obtained. For items positioned in the room, a weighing platform as used in furniture calorimeters can be used and has been successfully applied.

6   Extended calculations

6.1   Filling time of room and hood

At the beginning of a test there is some delay time in order to fill the part above the soffit level of the door in the room. Filling of the hood in the beginning of the test is almost negligible since the smoke gases will enter immediately into the duct. Some filling of the hood might occur later on in the test if the extraction rate is close to the limit of the system. This is close to flashover conditions if the maximum exhaust flow rate is used. Delay time correction can be easily incorporated into the time shifting of the data.

Although mixing of the gases is enhanced by the baffle plates into the hood, corrections can be made to take into account mixing of the gases. However, this will only be necessary if one wants to perform calculations which are better than the actual accuracy as given in ISO 9705. The following formulae developed by Kokkala can be used for correction of mixing [2]:

$$C_m(t) = C_{r,max}[\exp(-t/t_d) - \exp(t/\tau_m)]/(1-\tau')$$

where

C_m is the measured concentration;

$C_{r,max}$ is the maximum concentration;

τ' is the dimensionless time constant = $\dfrac{\tau_m}{t_d}$

τ_m is the time constant of mixing = volume of "mixing chamber" (V)/volume flow rate ($\dot{V}$);

t_d is the duration time of phenomena (s).

6.2 Prediction of mass flow and interface position

6.2.1 General equations

General equations for the vent flow rates as a function of temperature profiles are described in this subclause. The equations are based on the orifice concept.

Flows in and out of the compartment are driven by pressure differences across the vent. Inside the compartment, velocities are negligible except locally in flames, plumes and wall jets. Thus, (static) pressure varies vertically only due to gravity. The velocity at height z is given according to Bernouilli's equation [10] as

$$v(z) = \pm C\sqrt{2\frac{|p_i(z) - p_\infty(z)|}{\rho_d(z)}} \tag{1}$$

where

v is the velocity (m·s^{-1});

C is the orifice coefficient;

p_i is the pressure inside the compartment (Pa);

p_∞ is the pressure outside the compartment (Pa);

z is the height above floor level (m);

ρ_d is the density of gases in the doorway (kg·m^{-3}).

The height z_n at which there is no pressure difference (and no flow) between the compartment and the environment, is called the neutral plane. There is a maximum of one neutral plane for the case of a room connected to the outside (or a large reservoir). Hydrostatic pressure outside the compartment can be written as a function of height:

$$p_\infty(z) = p(z_n) + (z_n - z)\rho_\infty g \tag{2}$$

11

where

ρ_∞ is the density of ambient air (kg·m^{-3});

g is the acceleration due to gravity (m·s^{-2}).

Hydrostatic pressure differences are very small (typically a few pascals) compared to the magnitude of the absolute pressure itself, which is of the order of 10^5 Pa. Therefore, p_∞ may be written as

$$\rho_\infty = \frac{\rho_{\text{ref}} T_{\text{ref}}}{T_\infty} = \frac{352{,}8}{T_\infty} \tag{3}$$

where

ρ_{ref} is the density of ambient air at temperature T_{ref} and atmospheric pressure (kg·m^{-3});

T_{ref} is the reference temperature (K);

T_∞ is the temperature of ambient air (K).

With acceleration of gravity $g = 9{,}81$ m·s^{-2}, equation (2) then becomes

$$p_\infty(z) = p(z_n) + (z_n - z)\frac{3\,461}{T_\infty} \tag{4}$$

Inside the compartment, temperature is not constant with height. Thus, pressure as a function of height follows from

$$p_i(z) = p(z_n) + \int_0^{z - z_n} \frac{3\,461}{T_i(z')}\,\mathrm{d}'z \tag{5}$$

Combining equations (4) and (5) leads to the following expression for the pressure difference:

$$\Delta p(z) = 3\,461 \int_0^{z - z_n} \left(\frac{1}{T_i(z')} - \frac{1}{T_\infty} \right)\mathrm{d}'z \tag{6}$$

The mass flow rate out of the compartment follows from integration of equation (1):

$$\dot{m}_o = C_o W_d \int_0^{H_d - z_n} \rho_d(z')v(z')\,\mathrm{d}'z = C_o W_d \int_0^{H_d - z_n} \sqrt{2\rho_d(z')\Delta p(z')}\;\mathrm{d}'z \tag{7}$$

where

W_d is the door width (m);

H_d is the door height (m).

As the outflowing gases mainly consist of nitrogen, the density is not too different from that for air at the same temperature and pressure. Substitution of equation (6) and an expression analogous to equation (3) for ρ_d into equation (7) yields

$$\dot{m}_o = 1\,563\,C_o W_d \int\limits_0^{H_d - z_n} \left[\frac{1}{T_d(z')} \int\limits_0^{z' - z_n} \left(\frac{1}{T_\infty} - \frac{1}{T_i(z'')} \right) dz'' \right]^{1/2} d'z \tag{8}$$

Similarly, the inflow rate is equal to

$$\dot{m}_i = 1\,563\,C_i W_d \int\limits_0^{z_n} \left[\frac{1}{T_d(z')} \int\limits_0^{z' - z_n} \left(\frac{1}{T_\infty} - \frac{1}{T_i(z'')} \right) dz'' \right]^{1/2} d'z \tag{9}$$

It should be noted that a distinction is made between the orifice coefficient for inflow C_i and that for outflow C_o. This allows implementation of the recommendations in reference [11].

6.2.2 z_n from temperature profiles and one Δp measurement

Algorithms developed at NIST to reduce room fire data include a procedure to obtain z_n and mass flow rates through the vent [12]. These algorithms are referred to as RAPID. Equation (6) shows that Δp can be calculated as a function of height on the basis of the temperature profile measured inside the room if z_n is known. The NIST RAPID procedure [12] requires measurement of Δp at one reference height z_{ref} in addition to the temperature profile inside the room. z_n can then be found by evaluating equation (6) at z_{ref}:

$$\Delta p(z_{ref}) = 3\,461 \int\limits_0^{z_{ref} - z_n} \left(\frac{1}{T_i(z')} - \frac{1}{T_\infty} \right) d'z \tag{10}$$

The best reference height is at the soffit as the pressure difference is usually the largest at this height. Once z_n is known, mass flow rates can be obtained according to equations (8) and (9). This also requires the temperature profile in the doorway.

6.2.3 z_n via temperature profiles only

The RAPID procedure outlined in 6.2.2 has some practical difficulties. $\Delta p(z_{ref})$ is in the order of a few pascals and is very difficult to measure. Moreover, pressure data at such a low level are very noisy mainly due to turbulence. Another important drawback of the procedure is that it does not necessarily conserve mass. Therefore, a procedure is outlined here, based on temperature profiles only [6]. The requirement for conservation of mass replaces equation (10) as the equation for obtaining z_n. The mass balance equation has the following form:

$$\frac{dm_r}{dt} = \dot{m}_i + \dot{m}_b + \dot{m}_v - \dot{m}_o \tag{11}$$

where

m_r is the mass accumulated inside the compartment (kg);

$\dot{m}_i$ is the ignition source mass flow rate (kg/s).

The rate of change of mass inside the room can be calculated from the temperature profile measured inside the room via

$$\frac{dm_r}{dt} = 352{,}8\,WL \frac{d}{dt} \int\limits_0^H \frac{d'z}{T_i(z')} \tag{12}$$

where

W is the room width (m);

L is the room length (m);

H is the room height (m).

The burner gas flow rate $\dot{m}_b$ is measured. $\dot{m}_v$ consists of water vapour and pyrolysis gases emerging from the walls. Both $\dot{m}_b$ and $\dot{m}_v$ are usually very small compared to the other terms in equation (12) and can be neglected. $\dot{m}_o$ and $\dot{m}_i$ are functions of z_n as indicated in equations (8) and (9). Therefore, equation (11) is a non-linear equation in z_n which can be solved iteratively.

6.3   Estimate of sample mass loss

When no mass loss measurements are made during tests it is possible to estimate the mass loss rate as a function of time using one of two methods. The first method is to divide the measured heat release by an effective heat of combustion of the product, which might be determined, for example, in the cone calorimeter. The second method is to estimate the mass loss rate by means of the gas analysis measurements. A procedure for this method is outlined in annex C [13].

6.4   Fire growth models

The test results of a room corner test may be predicted by means of a simulation model which calculates wall fire growth in a small room. An extensive overview of modelling full-scale test results is given in ISO/TR 11696. Fundamental solutions for fire growth need to address various phenomena such as heat transfer, fluid dynamics and combustion. Most of the developed models have introduced some simplifications for those problems.

They can be divided into a number of categories, as follows.

— Models applying straightforward empirical or statistical methods and using small scale data obtained directly from one or more test methods such as the cone calorimeter (ISO 5660) and the LIFT apparatus. Although they use a considerable number of simplifications, their predictions have been successful. Most of them are limited to one specific scenario, but extensions to other scenarios are possible by using other empirical parameters.

— Models applying semi-material characteristics. These semi-material characteristics are calculated from the small scale data obtained in, for example, the cone calorimeter (ISO 5660) and the LIFT apparatus and can be considered as a derivative or mean value of a fundamental material characteristic. Examples of such characteristics are mean $k\rho\,c$, ignition temperature, etc. Most of these models also show satisfactory results and are applicable for more than one scenario.

— Models applying fundamental material characteristics. Most of these models use characteristics which are less easy to determine with standard reaction to fire apparatuses, but some progress has been made in recent years. They have, however, been limited to certain products. In most cases these are sub-models describing one type of flame spread (e.g. horizontal flame spread) and they must be incorporated in a zone on field model.

For a description of the different developed models see ISO/TR 11696.

7   Precision data

7.1   General

Two round robins on the room corner test have been conducted in recent years. First, an initial round robin with five laboratories was carried out prior to the circulation of ISO/DIS 9705 [14]. This first round robin used the standard

procedure as described in the standard. Later, a wider round robin was carried out as a joint activity between ISO and ASTM but using the ASTM procedure as testing protocol, i.e. the alternative ignition source with only the walls covered [15]. The results of the round robins are given in 7.2 and 7.3.

7.2   ISO round robin

This round robin was performed at five laboratories in Denmark, Finland, Norway, Sweden and the United Kingdom. The results are given in Tables 3 to 6 and indicate that the reproducibility of the method is similar to other fire test methods, such as fire resistance tests using large-scale furnaces. The 95 % confidence interval of the mean of the time to flashover was found to be ± 37 s and ± 18 s for ordinary plywood and melamine-faced particle-board, respectively. A similar range was found also for the rates of smoke and CO production. The reproducibility of the tests on the fire-retarded plywood was about the same as the untreated plywood, although in only one of the tests flashover conditions were reached.

The results of the tests on the fire retarded expanded polystyrene varied considerably, mainly due to the different gluing methods.

Table 3 — Results for birch plywood

Laboratory	Time to reach			
	Rate of heat release = 1 MW	Rate of smoke production = 40 m²/s	Rate of CO production = 15 g/s	Heat flux = 20 kW/m²
VTT	137 s	129 s	121 s	153 s
SINTEF NBL	152 s	129 s	120 s	
RW	122 s	121 s	112 s	138 s
FRS	209 s	198 s		
Average	137 s[a]	126 s[a]	118 s	146 s
Confidence interval (95 %)	± 37 s	± 11 s[a]	± 12 s	
[a] FRS results are not included, because the time to critical smoke value indicated that the test was an outlier according to Dixon's outlier test [11] (see also Appendix 3 of [11]).				

Table 4 — Results for melamine-faced particle-board

Laboratory	Time to reach			
	Rate of heat release = 1 MW	Rate of smoke production = 40 m²/s	Rate of CO production = 15 g/s	Heat flux = 20 kW/m²
VTT	182 s	158 s	172 s	190 s
SP	204 s	174 s	198 s	
RW	202 s	165 s	174 s	208 s
FRS	206 s	186 s		
Average	199 s	171 s	181 s	199 s
Confidence interval (95 %)	± 18 s	± 19 s	± 36 s	

Table 5 — Results for fire-retarded plywood

Laboratory	Time to reach			
	Rate of heat release = 1 MW	Rate of heat release = 700 kW	Rate of CO production = 10 g/s	Heat flux = 10 kW/m^2
VTT	—	629 s	627 s	621 s
RW	1148 s	624 s	630 s	624 s
RW	—	645 s	657 s	630 s
FRS	—	637 s		
Average	—	634 s	638 s	625 s
Confidence interval (95 %)		± 15 s	± 41 s	± 5 s
NOTE The critical values are different in Tables 5 and 6.				

Table 6 — Results for fire-retarded polystyrene

Laboratory	Time to reach			
	Rate of heat release = 1 MW	Rate of smoke production = 40 m^2/s	Rate of CO production = 15 g/s	Heat flux = 10 kW/m^2
VTT	—	120 s	—	—
SP	67 s	59 s	79 s	55 s
SINTEF NBL	—	120 s	—	—
Average	—	100 s	—	—
NOTE The results of SP are different because of difference in glueing.				

7.3   ASTM round robin

During and after the publication of ISO 9705:1993, a second major round robin was conducted as a joint activity between ISO and ASTM. This study involved 12 laboratories throughout the world and seven lining products. The scenario for this round robin differed substantially from the European round robin. In the ASTM round robin, only the walls were covered with the testing material and the alternative ignition source was used with a different heat source programme than in the European round robin (40 kW to 160 kW). The measurements of heat release rate, room and doorway temperatures and floor heat flux showed the best results. Smoke measurements had more variations. As with all fire tests, the performance of the material, such as melting, delamination, etc., tended to influence the spread of the results. Overall repeatability levels according to ISO 5725 varied between 27 % and 33 % and overall reproducibility are varying between 29 % and 41 %. In terms of overall material performance, the round robin was successful. All materials that did not go to flashover performed the same in all tests at all laboratories. The same is valid for the materials which went to flashover. Therefore, attainment of flashover or reaching an HRR of 1 MW could be used as a criterion when the test is to be used for regulatory purposes.

8   Other test protocols using similar equipment

Several test protocols similar to ISO 9705:1993 or using the same test equipment, have been introduced in either national standards or in test programmes and for products other than wall linings. An overview of the different procedures is given in annex D.

9   Specimen mounting

In the test set-up of ISO 9705:1993, it is advised that both wall and ceiling linings be covered with material. Tests where only the walls are covered can be performed, but it should be noted that this is not the standard specimen configuration.

ISO 9705 requires that the mounting which is used in practice should be followed as much as possible. This is given in detail in clause 11 of ISO 9705:1993. When the material is mounted with an air gap, this air gap may be achieved by a steel framework on which the material is mounted.

The mounting method most frequently used in practice should be used in the text procedure. When this is not the case, it should be clearly stated and reasons for alternative mounting should be explained.

Annex A

Calculation of HRR by means of different gas analysis data

A.1 General equations

A.1.1 Only O_2 is measured

In this case all water vapour (by a cooling unit and a moisture sorbent) and CO_2 (by a chemical sorbent) must be removed from the sample stream before O_2 is measured. This leads to the assumption that the sample gas only consists of O_2 and N_2. This is approximately true provided CO production is negligible. The mole fraction of O_2 in the oxygen analyser prior to a test can be written as

$$X_{O_2}^{A^o} = \frac{\dfrac{\dot{m}_{O_2}^o}{M_{O_2}}}{\dfrac{\dot{m}_{O_2}^o}{M_{O_2}} + \dfrac{\dot{m}_{N_2}^o}{M_{N_2}}} \qquad (A.1)$$

where

$X_{O_2}^{A^o}$ is the measured mole fraction of O_2;

$\dot{m}_{O_2}^o$ is the mass flow rate of O_2 in the incoming air (kg/s);

M_{O_2} is the molecular mass of O_2 (approx. 32 kg/kmol);

M_{N_2} is the molecular mass of N_2 (approx. 28 kg/kmol);

$\dot{m}_{N_2}^o$ is the mass flow rate of N_2 in the incoming air (kg/s).

Equation (A.1) depends on the assumption that prior to the test the ratio of the mass flow of O_2 to the mass flow of N_2 is the same in the oxygen analyser as it is in the incoming air. It is then assumed that the composition of the incoming air does not change during a test.

Likewise, the mole fraction of O_2 in the analyser during the test is given by

$$X_{O_2}^{A} = \frac{\dfrac{\dot{m}_{O_2}}{M_{O_2}}}{\dfrac{\dot{m}_{O_2}}{M_{O_2}} + \dfrac{\dot{m}_{N_2}}{M_{N_2}}} \qquad (A.2)$$

where it is again assumed that the ratio of the mass flow of N_2 and O_2 are the same as they are in the exhaust duct.

The nomenclature is similar to that of equation (A.1) with the exception that superscript º is omitted as everything relates to the exhaust gases rather than to the incoming air. By rearranging equations (A.1) and (A.2) and using the oxygen principle, the rate of heat release is given by:

$$\dot{q} = E\left[\frac{X_{O_2}^{A^o} - X_{O_2}^{A}}{1 - X_{O_2}^{A}}\right] \dot{m}_a \frac{M_{O_2}}{M_a}\left(1 - X_{H_2O}^{o} - X_{CO_2}^{o}\right) \tag{A.3}$$

where

$\dot{q}$ is the rate of heat release (kW);

E is the heat released per O_2 consumed (13,1 MJ/kg of O_2);

M_a is the molecular mass of the incoming air (kg/kmol);

$\dot{m}_a$ is the mass flow rate of the incoming air (kg/s);

$X_{H_2O}^{o}$ is the mole fraction of H_2O in the incoming air;

$X_{CO_2}^{o}$ is the mole fraction of CO_2 in the incoming air.

If no CO_2 analyser is present, $X_{CO_2}^{o}$ is not measured. However, it is assumed that ambient air is drawn in for combustion. $X_{CO_2}^{o}$ is then approximately constant and negligible (approx. 330 ppm).

It is furthermore assumed that even if no water vapour analyser is present, moisture content of the incoming air is known. If the air is at temperature T_a, pressure p_a and has a relative humidity of RH %, the mole fraction of water vapour in the incoming air follows from

$$X_{H_2O}^{o} = \frac{RH}{100} \times \frac{p_s(T_a)}{p_a} \tag{A.4}$$

with

RH is the relative humidity (%);

$p_s(T_a)$ is the saturation pressure of water vapour at T_a (Pa);

T_a is the air temperature (K);

p_a is the air pressure (Pa).

The saturation pressure p_s as a function of T_a is shown in Figure A.1. A curve fit in the range of 0 °C < T_a < 0 °C is also given. The fit has the functional form of a solution to the Clausius-Clapeyron equation suggested by Antoine back in 1888.
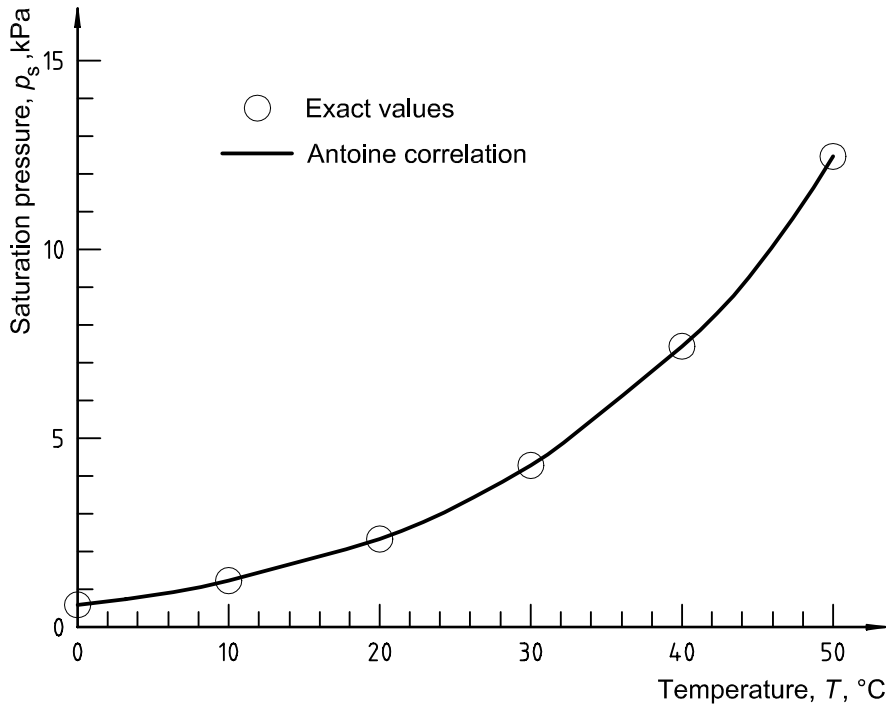
$\ln (p_s) = C_0 - C_1/(C_2 + T)$; $C_0 = 23,2$; $C_1 = 3\ 816$; $C_2 = -46$

Figure A.1 — Saturation pressure as a function of temperature

$X^o_{H_2O}$ can also be determined experimentally by temporarily by-passing the water vapour trap prior to a test. Oxygen concentration measured with and without the trap can then be substituted into the following equation:

$$\left[X^{A^0}_{O_2} \right]_{without\ trap} = \left(1 - X^o_{H_2O}\right)\left[X^{A^0}_{O_2} \right]_{with\ trap} \tag{A.5}$$

Once $X^o_{H_2O}$ is known, the molecular mass of the incoming air follows from:

$$M_a = M_{dry}\left(1 - X^o_{H_2O}\right) + M_{H_2O}\ X^o_{H_2O} \tag{A.6}$$

where

M_{dry} is the molecular mass of dry air (approx. 29 kg/kmol);

M_{H_2O} is the molecular mass of H_2O (approx. 18 kg/kmol).

Unfortunately, in an open system, it is the flow rate in the exhaust duct that is measured, and not the incoming airflow rate. In order to find a relation between $\dot{m}_a$ and $\dot{m}_e$, the oxygen depletion factor ϕ is defined as

$$\phi = \frac{\dot{m}^o_{O_2} - \dot{m}_{O_2}}{\dot{m}^o_{O_2}} \tag{A.7}$$

The oxygen depletion factor ϕ is the fraction of the incoming air which is fully depleted of its oxygen. Via equations (A.1) and (A.2), ϕ can be rewritten as

$$\phi = \frac{X_{O_2}^{A\,o} - X_{O_2}^{A}}{\left(1 - X_{O_2}^{A}\right) X_{O_2}^{A\,o}} \tag{A.8}$$

Due to the combustion chemistry, the number of moles in the fraction of the air fully depleted of its oxygen is replaced by an equal or larger number of moles of combustion products (including N_2) in the exhaust flow. Defining the expansion factor α as the ratio of the two above-mentioned molar quantities, an expression linking $\dot{m}_a$ to $\dot{m}_e$ is given by

$$\frac{\dot{m}_e}{M_e} = \frac{\dot{m}_a}{M_a}(1 - \phi) + \frac{\dot{m}_a}{M_a}\alpha\phi \tag{A.9}$$

With $M_e \approx M_a$ (in absence of anything better) this can be simplified to

$$\dot{m}_a = \frac{\dot{m}_e}{1 + \phi(1 - \alpha)} \tag{A.10}$$

As the composition of the fuel is usually not known, some average value has to be used for α. Complete combustion of pure carbon in dry air results in $\alpha = 1$. If the fuel is pure hydrogen, α is equal to 1,21. A recommended average value for α is 1,105, which is correct for methane. The final equation for this case now follows from equations (A.3), (A.8) and (A.10):

$$\dot{q} = E \frac{\phi}{1 + \phi(\alpha - 1)} \dot{m}_e \frac{M_{O_2}}{M_a}\left(1 - X_{H_2O}^{o} - X_{CO_2}^{o}\right) X_{O_2}^{A\,o} \tag{A.11}$$

Equation (A.11) is expected to be accurate to within ± 10 % provided combustion is complete, i.e., all of the carbon is converted to CO_2. The errors will be larger if CO or soot production is considerable or if a significant amount of the combustion products is other than CO_2 and H_2O (e.g. HCl).

A.1.2 O_2 and CO_2 are measured

This case is similar to that covered in the previous subclause. It is now assumed that only water vapour is trapped before the sample reaches the gas analysers. Again, the equations are derived on the basis of conservation of nitrogen. The relation between $\dot{m}_{O_2}^{o}$, $\dot{m}_{O_2}$ $\dot{m}_{N_2}$ is now given by

$$\dot{m}_{O_2}^{o} = \frac{X_{O_2}^{A\,o}}{1 - X_{O_2}^{A\,o} - X_{CO_2}^{A\,o}} \frac{M_{O_2}}{M_{N_2}} \dot{m}_{N_2} \tag{A.12}$$

$$\dot{m}_{O_2} = \frac{X_{O_2}^{A}}{1 - X_{O_2}^{A} - X_{CO_2}^{A}} \frac{M_{O_2}}{M_{N_2}} \dot{m}_{N_2} \tag{A.13}$$

where

$X_{CO_2}^{A\,o}$ is the measured mole fraction of CO_2 in the incoming air;

$X_{CO_2}^{A}$ is the measured mole fraction of CO_2 in the exhaust gases.

The mole fraction of CO_2 in the incoming air is generally very small and around 330 ppm. The rate of heat release is again given by equation (A.11). However, ϕ is now slightly different and follows from equations (A.7), (A.12) and (A.13):

$$\phi = \frac{X_{O_2}^{A^o}\left(1-X_{CO_2}^{A}\right)-X_{O_2}^{A}\left(1-X_{CO_2}^{A^o}\right)}{\left(1-X_{O_2}^{A}-X_{CO_2}^{A}\right)X_{O_2}^{A^o}}$$ (A.14)

Again, the equation is accurate within $\pm\,10\,\%$ provided combustion is complete.

A.1.3 O_2, CO_2 and CO are measured

This case is identical to that covered in the last subclause if the CO production is negligible.

Taking CO into account, ϕ is now given by

$$\phi = \frac{X_{O_2}^{A^o}\left(1-X_{CO_2}^{A}-X_{CO}^{A}\right)-X_{O_2}^{A}\left(1-X_{CO_2}^{A^o}\right)}{\left(1-X_{O_2}^{A}-X_{CO_2}^{A}-X_{CO}^{A}\right)X_{O_2}^{A^o}}$$ (A.15)

where

X_{CO}^{A} is the measured mole fraction of CO in the exhaust gases.

However, if at some point during a test significant amounts of CO are produced, a correction has to be made to equation (A.11) as E is based on the assumption that combustion is complete. This correction is derived below.

First, assume for the purpose of this derivation that all of the CO is converted to CO_2 in a hypothetical catalyser in the exhaust duct, downstream of the sampling point. The amount of O_2 consumed in this catalyser with ϕ according to equation (A.15) is given by

$$\left(\Delta\dot{m}_{O_2}\right)_{cat} = \frac{1}{2}\dot{m}_{CO}\frac{M_{O_2}}{M_{CO}} = \frac{1}{2}\dot{m}_{O_2}\frac{X_{CO}^{A}}{X_{O_2}^{A}} = \frac{1}{2}(1-\phi)\frac{X_{CO}^{A}}{X_{O_2}^{A}}\frac{M_{O_2}}{M_a}\dot{m}_a X_{O_2}^{o}$$ (A.16)

where

$\dot{m}_{CO}$ is the mass flow rate of CO at the sampling point (kg/s);

M_{CO} is the molecular mass of CO (≈ 28 kg/kmol).

The rate of heat release downstream of the catalyser is given by

$$\dot{q}_{tot} = E\left[\dot{m}_{O_2}^{o}-\dot{m}_{O_2}+\left(\Delta\dot{m}_{O_2}\right)_{cat}\right]$$ (A.17)

where $\dot{q}_{tot}$ is the total heat release downstream of the catalyser.

The rate of heat released in the catalyser by combustion of CO to CO_2 is equal to

$$\dot{q}_{cat} = \left(\Delta\dot{m}_{O_2}\right)_{cat}E_{CO}$$ (A.18)

where

E_{CO} is the net heat release per unit mass of O_2 consumed for combustion of CO to CO_2 ($\approx 17,6$ MJ/kg of O_2).

Thus, according to Hess' law, the rate of heat release at the sampling point is

$$\dot{q} = \dot{q}_{tot} \ - \ \dot{q}_{cat} = E\left(\dot{m}_{O_2}^o - \ \dot{m}_{O_2}\right) \ - \ \left(E_{CO} \ - \ E\right)\left(\Delta\dot{m}_{O_2}\right)_{cat} \tag{A.19}$$

This equation can be transformed with equations (A.15) and (A.16) to the final form:

$$\dot{q} = \left[E\phi - \left(E_{CO} - E\right)\frac{1-\phi}{2}\frac{X_{CO}^A}{X_{O_2}^A}\right]\frac{\dot{m}_e}{1+\phi(\alpha - 1)}\frac{M_{O_2}}{M_a}\left(1 - X_{H_2O}^o\right)X_{O_2}^{Ao} \tag{A.20}$$

A.1.4 O_2, CO_2, CO and H_2O are measured

O_2, CO_2, CO, H_2O and N_2 make up for over 99 % of the exhaust gases in almost all full-scale fire tests. Consequently, it is assumed that these are the only species in the exhaust gas flow. With this assumption, the availability of the H_2O measurement simplifies the analysis and improves accuracy. The mass flow rates of all species in the exhaust duct can now be written directly as a function of $\dot{m}_e$:

$$\dot{m}_{O_2} = \left(1 - X_{H_2O}\right)X_{O_2}^A\frac{M_{O_2}}{M_e}\dot{m}_e \tag{A.21}$$

$$\dot{m}_{CO_2} = \left(1 - X_{H_2O}\right)X_{CO_2}^A\frac{M_{CO_2}}{M_e}\dot{m}_e \tag{A.22}$$

$$\dot{m}_{CO} = \left(1 - X_{H_2O}\right)X_{CO}^A\frac{M_{CO}}{M_e}\dot{m}_e \tag{A.23}$$

$$\dot{m}_{H_2O} = X_{H_2O}\frac{M_{H_2O}}{M_e}\dot{m}_e \tag{A.24}$$

$$\dot{m}_{N_2} = \left(1 - X_{H_2O}\right)\left(1 - X_{O_2}^A - X_{CO_2}^A - X_{CO}^A\right)\frac{M_{N_2}}{M_e}\dot{m}_e \tag{A.25}$$

The molecular mass of the exhaust gases M_e can be found by setting the sum of equations (A.21) to (A.25) equal to $\dot{m}_e$. Substitution of numerical values for the molecular masses of the various species yields

$$M_e = 18 + 4\left(1 - X_{H_2O}\right)\left(X_{O_2}^A + 4X_{CO_2}^A + 2,5\right) \tag{A.26}$$

Since the flow equations in ISO 9705 are based on the assumption that the exhaust gases have the same density as dry air, use of M_e leads to more accurate equations for the mass flow rate. For an orifice plate, the flow equation is replaced by

$$\dot{m}_e = C\sqrt{\frac{M_{dry}}{M_eT_e}\Delta p} \tag{A.27}$$

For the case of a bi-directional probe, the flow equation is replaced by

$$\dot{m}_e = 26,54\frac{Ak_c}{f(Re)}\sqrt{\frac{M_{dry}}{M_eT_e}\Delta p} \tag{A.28}$$

The mass flow rate of air entering the system may now be calculated as a function of $\dot{m}_e$ on the basis of conservation of nitrogen. Combination of equation (A.25) and a similar equation linking $\dot{m}_a$ to $\dot{m}_{N_2}$ results in

$$\frac{\dot{m}_a}{M_a} = \frac{\left(1 - X_{H_2O}\right)\left(1 - X_{O_2}^A - X_{CO_2}^A - X_{CO}^A\right)}{\left(1 - X_{H_2O}^o\right)\left(1 - X_{O_2}^{Ao} - X_{CO_2}^{Ao}\right)} \frac{\dot{m}_e}{M_e} \tag{A.29}$$

The molecular mass of the incoming air follows from equation (A.6). The mass flow rate of oxygen into the system can now be calculated from equation (A.29) as

$$\dot{m}_{O_2}^o = \frac{\left(1 - X_{H_2O}\right)\left(1 - X_{O_2}^A - X_{CO_2}^A - X_{CO}^A\right)}{1 - X_{O_2}^{Ao} - X_{CO_2}^{Ao}} X_{O_2}^{Ao} \frac{M_{O_2}}{M_e} \dot{m}_e \tag{A.30}$$

The O_2 depletion factor ϕ is obtained by substituting equations (A.21) and (A.30) into equation (A.8)

$$\phi = \frac{X_{O_2}^{Ao}\left(1 - X_{CO_2}^A - X_{CO}^A\right) - X_{O_2}^A\left(1 - X_{CO_2}^{Ao}\right)}{\left(1 - X_{O_2}^A - X_{CO_2}^A - X_{CO}^A\right) X_{O_2}^{Ao}} \tag{A.31}$$

This equation is identical to the one derived in (A.15). A correction can be found for incomplete combustion in a similar way as developed there. The final form of the equation for rate of heat release is then given by

$$\dot{q} = \left[E\phi - \left(E_{CO} - E\right)\frac{1-\phi}{2}\frac{X_{CO}^A}{X_{O_2}^A}\right]\frac{M_{O_2}}{M_a}\dot{m}_a\left(1 - X_{H_2O}^o\right)X_{O_2}^{Ao} \tag{A.32}$$

A.2 Net heat release

Often in full-scale fire tests, specimens are exposed to an ignition source such as a gas burner or a wood crib. It should be noted that $\dot{q}_{net}$, the rate of heat release from the specimen only, can be interesting. In such tests, part of the oxygen depletion in the exhaust duct is due to combustion of the ignition source fuel. This part must be subtracted from the total O_2 depletion in order to determine $\dot{q}_{net}$ released by the specimen.

The case of a gas burner ignition source is considered first. The flow rate of fuel gas to the burner $\dot{m}_g$ is usually measured and combustion efficiency χ for a gas may assumed to be 100 %. Under these conditions, the oxygen depletion due to combustion of the burner gas is given by

$$\left(\Delta\dot{m}_{O_2}\right)_g = \frac{\dot{m}_g\left(\Delta h_c\right)_g}{E_g} \tag{A.33}$$

where

$(\Delta\dot{m}_{O_2})_g$ is the O_2 depletion due to combustion of the gas (kg/s);

$\dot{m}_g$ is the mass flow rate to the burner (kg/s);

$(\Delta h_c)_g$ is the net heat of combustion of the gas (46,4 MJ/kg for C_3H_8);

E_g is the net heat released per unit mass of O_2 consumed for combustion of the burner gas (12,76 MJ/kg for C_3H_8).

Thus, the net rate of heat release by the specimen follows from subtracting $E(\Delta\dot{m}_{O_2})_g$ from $\dot{q}$ calculated according to equation (A.11), (A.20) or (A.32).

Although this procedure is straightforward, there is a problem in practical applications. The problem is related to the delay in response of the instrumentation in the exhaust duct. The delay consists partly of the time required by the combustion products to travel from the fire to the measuring point. This transport time can easily be taken into account by shifting the measurements over the appropriate transport time interval. However, a considerable part of the delay is usually much more difficult to correct and is due to filling of an enclosure, response time of gas analysers etc.

In cases where the latter part of the delay turns out to be significant, a better procedure to determine $\dot{q}_{net}$ may consist of running a calibration test with the ignition source and a non-combustible specimen. Such a test yields a baseline rate of heat release curve. For subsequent tests, $\dot{q}_{net}$ is determined by subtracting the baseline from the HRR obtained via (A.11), (A.20) or (A.32). The same procedure may be used for ignition sources with unknown heat of combustion or unknown combustion efficiency, such as wood cribs.

A.3 Summary of calculation procedures

Depending on the configuration of gas analysers and the type of flow rate measurement, different procedures should be used to calculate the rate of heat release. With the most common instrumentation the recommended procedure consists of the following steps.

Calculate M_e according to equation (A.26).

Calculate $\dot{m}_e$ according to equation (A.28).

Calculate $\dot{m}_a / M_a$ according to equation (A.29).

Calculate ϕ according to equation (A.15).

Calculate $\dot{q}$ according to equation (A.32).

When all tests are conducted with a gas burner ignition source, $\dot{q}_{net}$ may be calculated as indicated in clause A.2. Note that the mass flow rates of CO_2, CO and H_2O in the exhaust can be calculated from equations (A.22) to (A.24). To obtain the mass flow rates generated by combustion, however, the flow rate of CO_2 and H_2O in the incoming air must be subtracted from equation (A.22) and equation (A.24) respectively. These can be obtained from

$$\dot{m}^o_{H_2O} = X^o_{H_2O}\frac{M_{H_2O}}{M_a}\dot{m}_a \qquad\qquad\qquad (A.34)$$

$$\dot{m}^o_{CO_2} = \left(1 - X^o_{H_2O}\right)X^{Ao}_{CO_2}\frac{M_{CO_2}}{M_a}\dot{m}_a \qquad\qquad\qquad (A.35)$$

By multiplying the generation rates of CO_2 and CO by the appropriate mass ratio, the generation rate of carbon may be calculated. Furthermore, if the carbon to hydrogen ratio of the fuel volatiles is known, this may be used to estimate the mass loss rate of the fuel. The contribution from an ignition source can be subtracted in a similar way as explained in A.2 for the rate of heat release.

Annex B

Practical example of the measurements of toxic gases by FTIR and ion chromatography

B.1 Description of the FTIR measurement technique

A complete description of the testing method is given in NT FIRE 047 [42]. The principle of this method can be explained as follows.

Smoke gas samples for the FTIR analysis are taken from a gas sampling line connected to the test apparatus (usually the exhaust duct). The gas sample is drawn continuously through a heated sampling line to a heated IR absorption cell of a FTIR spectrometer. The infrared beam is directed from the interferometer through the gas absorption cell; at chosen intervals, interferograms are acquired and after the test converted to absorption spectra.

The sampling line and the IR absorption cell are heated to keep the smoke gas composition unchanged for the analysis. At the elevated temperature of over 120 °C water is prevented from liquefying, gases soluble in water [e.g. hydrogen cyanide (HCN) and hydrogen chloride (HCl), etc.] from dissolving and lightweight gases insoluble in water from precipitating.

Heating and filtering help to keep the sampling line clean and the IR absorption cell with mirrors inside.

FTIR is based on infrared absorption. Specific to FTIR is conversion of regular irradiance from an infrared source into interfered irradiance and conversion of an interferogram into a conventional wavelength spectrum with wide wavelength range. In this method, the spectrum is presented as absorbance (energy lost or absorbed in the optical path) as function of radiation in wave numbers (number of cycles per centimetre).
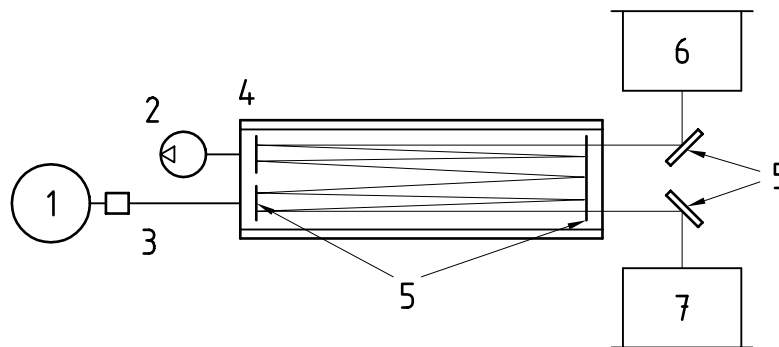
Key

1   Exhaust duct of fire test
2   Pump
3   Heated sampling line
4   Heated gas cell
5   Mirrors
6   IR Source
7   Detector

Figure B.1 — Schematic view of gas sampling and IR measurement

Polyatomic and heteronuclear diatomic compounds have absorption in the infrared region (O_2 has to be measured with other methods) and can be identified on basis of absorbance or absorbances characteristic (at characteristic

Not for Resale

wavelengths) to the compound. Concentrations are related to intensities of absorption. Concentrations can be calculated on the basis of areas of absorbances in the spectra of the unknown and reference gas mixtures with known concentrations of gases.

Concentrations of smoke gases as a function of time can be calculated from successive measurements at regular intervals (5 s to 10 s is suitable).

B.2 Description of the ion chromatography measurement technique

Chromatography is a chemical analysis method based on the separation of the different components in a mixture. This separation is done between a mobile phase, in which components are soluble, and a stationary phase, on which they can be delayed.

In ion chromatography, the stationary phase is an ion exchange resin and the mobile phase an ionic solution. Depending on the size, the charge and the polarizability of the component, it will be delayed more or less by the column.

Two of the essential measurement parameters are as follows.

The retention time (t_R): time between injection and exit of the column (top of the peak) for a given component. It depends on the nature of the mobile and the stationary phases.

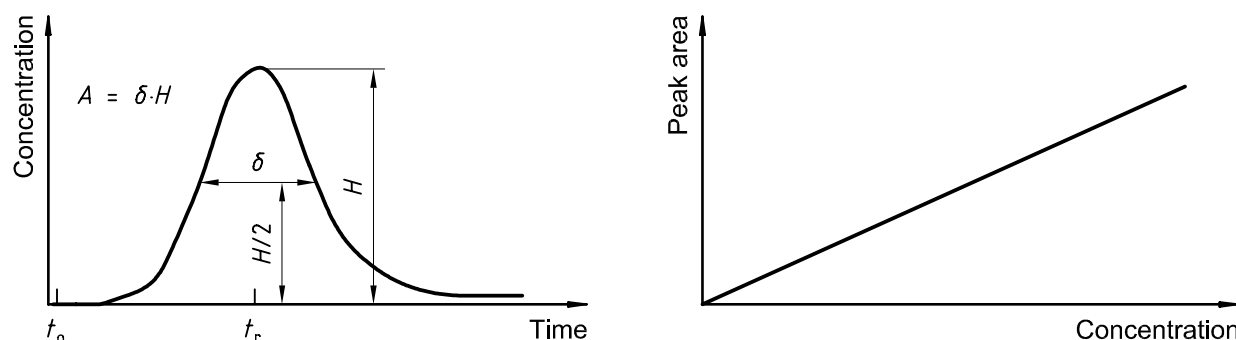The peak area (A): area between the baseline and the chromatogram, delimited by the start and the end of the peak.

Figure B.2 — Chromatographic parameters and calibration curve

A calibration curve is set up from injections of solutions containing the components to be analysed at known concentrations and gives peak area vs. concentration.

Several detection modes can be used, as follows.

a) The conductivity detection allows the analysis of HF, HCl, HBr, NO_2, SO_2. It is based on the ability for ionic solutions to carry current when placed between two different-charged electrodes. Conductivity is directly related to the concentration of the component by the formula given below:

$$C = kG = k\frac{1}{R}$$

where

C is the conductivity [Siemens];

R is the resistance [ohm]

G is the conductance [ohm^{-1}]

k is a constant (depends on the detection cell).

Species detected by conductivity are ionic, so this method requires a mobile phase containing strong electrolytes. Consequently, ionic analyses and ions of mobile phase can be detected. In order to avoid a loss of sensitivity of the detection due to the large quantity of ions from mobile phase, chemical suppression may be used. There are different systems but they all provide a lower baseline shift, a lower detection limit, and elimination of interference's from cautions (in case of anion analysis).

b)   Amperometry detection allows analysis of HCN. It is based on the measurement of the current generated by oxidation or reduction of a component on the surface of a working electrode. This current is proportional to the concentration of the component.

$$I = nFAD\delta^{-1}C$$

where

I is the current intensity [A];

n is the number of transferred electrons;

F is the Faraday constant [C mol^{-1})];
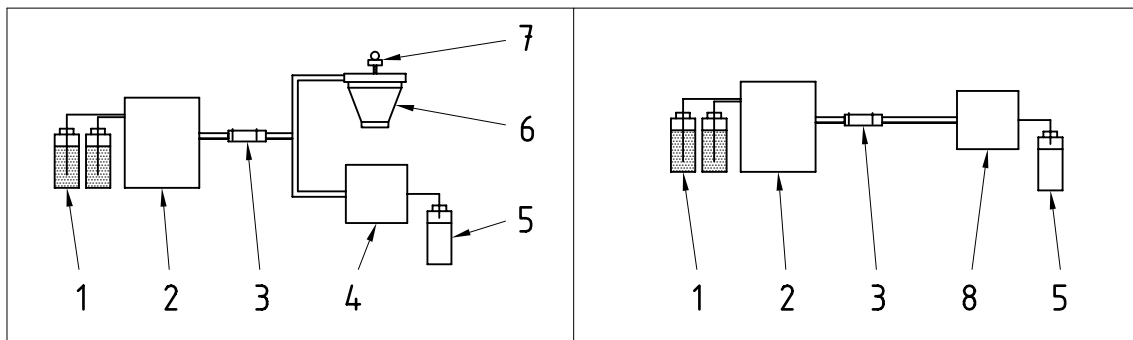
A is the electrode area [m^2];

D is the coefficient of diffusion [m^2 s^{-1}];

δ is the thickness of the detection cell [m];

C is the concentration of the component [mol l^{-1}].

For example, DC amperometry (direct current amperometry) can be used by applying a chosen and constant potential to the working electrode.

Key

1	Effluent	5	Waste
2	Pump	6	Chemical suppression
3	Column	7	Nitrogen
4	Conductimeter	8	Amperometer

Figure B.3 — Schematic view of conductivity and amperometry lines

B.3 Sampling line requirements for small- and large-scale testing

B.3.1 Sampling line description

B.3.1.1 Examples

Two sampling lines, one for the FTIR and one for the ion chromatography analysis can be used as described in the following practical example.

B.3.1.2 Probes

For measurement in the duct, two gas sampling probes can be fitted to the exhaust duct, as shown below.

⎯ The distance between the probes is 100 mm.

⎯ Between the gas sampling probes, a minimum of 15° offset should be foreseen.

⎯ One probe is connected to the FTIR sampling line, the second one to the ion chromatography sampling line. A filter is included in the FTIR sampling line.
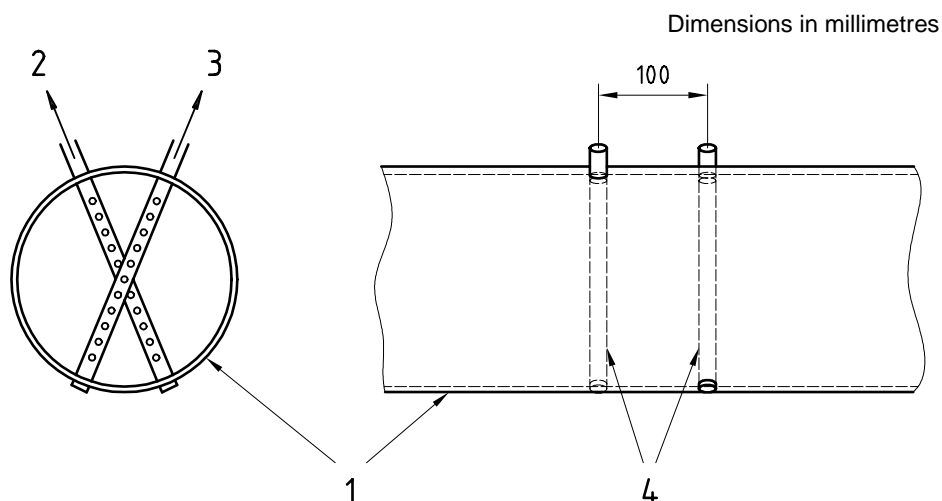
Key

1 Exhaust duct
2 Sample flow IC
3 Sample flow FTIR
4 Sample probes for FTIR and IC

Figure B.4 — Gas sampling probes position in the furniture and cone calorimeter exhaust duct
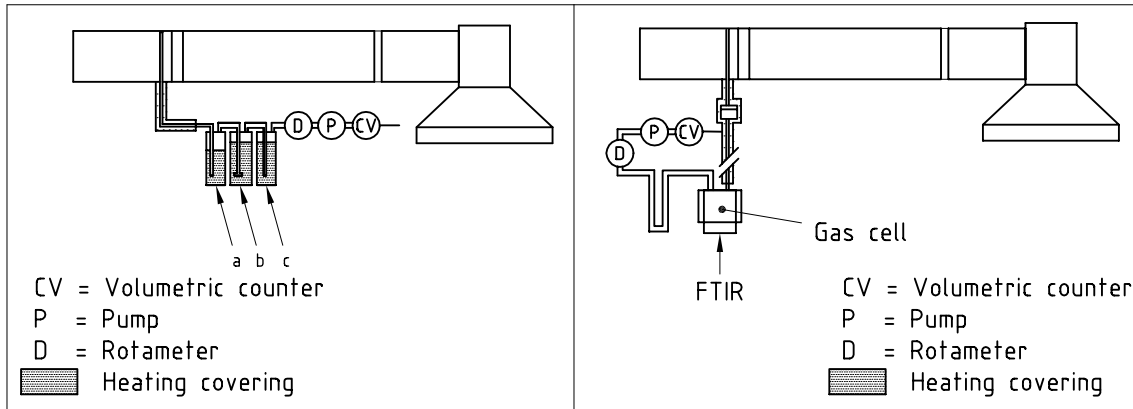
a   50 ml NaOH 0,1 M (straight head).

b   70 ml NaOH 0,1 M (sintered head).

c   70 ml NaOH 0,1 M (straight head).

Figure B.5 — Schematic view of FTIR and ion chromatography lines connections

For testing in accordance with an ISO 9705 room, the gas sampling probes can be installed as in Figure B.6.

Dimensions in millimetres
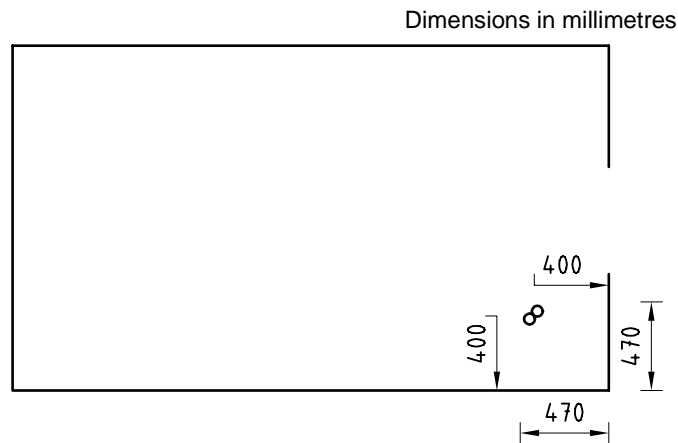
Figure B.6 — Horizontal position of gas sampling probes in the ISO 9705 room

B.3.1.3   Filter

In order to protect the FTIR analyser from soot and water, a filter unit has to be placed in the sampling lines between exhaust duct and FTIR line. This type of filter has to be inert regarding HCl, HBr or other gases of interest. To check its passivity property, it is necessary to analyse it after each test. Many types of filters may be used, but most laboratories adapt a stainless steel filter unit containing a glass fibre filter. An example of a commercial filter is "Whatman microfilter, 47 mm in diameter, multigrade 1µ GMF 150,47 mm in diameter".

B.3.1.4   Bubblers and bubbling solution

Three bubblers can be put in series. The nominal volume is 100 ml.

—   The first one is a straight bubbler, filled with 50 ml of 0,1M NaOH.

—   The second one is a sintered head bubbler (porosity 1), filled with 70 ml of 0,1M NaOH.

⎯ The third one, the guard bubbler, is a straight head bubbler (porosity 1), filled with 70 ml of 0,1M NaOH.

The two first bubblers are analysed together; the third one can be analysed separately to give information about the efficiency of the two first in trapping gases.

B.3.2 Conditions for the sampling lines

B.3.2.1 Heating of sampling line

Sampling lines should be heated at a temperature higher than 150 °C to avoid any condensation before analysis. This temperature is measured at filter level for FTIR line and at tubing level before bubblers for the ion chromatography line. This measurement has to be done with respective flow rate in the sampling lines.

B.3.2.2 Flow rates

The following flow rates can be utilized.

⎯ From 5 l/min to 10 l/min in the FTIR sampling line; the exact flow rate has to be chosen to meet the requirements of the response time.

⎯ From 2 l/min to 4 l/min in the ion chromatography sampling line; the exact flow rate has to be chosen depending on the type of bubblers.

Flow rates must be maintained during tests.

B.3.2.3 Procedures and instrumental requirements

For FTIR, the recommended resolution is between 2 cm^{-1} and 4 cm^{-1}. The response time of the analysis is 30 s or less and is checked according to the following procedure:

⎯ a known concentration of a calibration gas is introduced into the filter by the end of the sampling line;

⎯ time zero is the time when the recording of the FTIR values begins.

The response time value should indicate 90 % of the calibration gas concentration.

For ion chromatography, two chromatographic lines may be used:

⎯ conductivity line for HCl and HBr analysis;

⎯ amperometry line for HCN analysis.

Solutions from the two first bubblers are poured into a 200 ml calibrated flask. Bubblers walls are washed with fresh 0,1M NaOH solution. Final volume has to be adjusted to 200 ml. The flasks are kept at 4 °C until analysis.

Solutions from the guard bubbler are poured into a 100 ml calibrated flask. Bubbler walls are washed with fresh 0,1M NaOH solution. Final volume has to be adjusted to 100 ml. The flasks are kept at 4 °C until analysis.

Annex C

Estimation of mass loss rate by means of HRR and gas analysis measurements

When it is not possible to equip the test room with a load cell an indirect technique needs to be adopted using gas analysis data from the experiment. The method is outlined and summarized below [36].

Symbols:

f_Z yield of species Z, as determined from cone calorimeter measurements (kg Z/kg fuel)

k extinction coefficient measured in exhaust stack stream (m^{-1})

$\dot{m}$ mass loss rate of specimen and ignition source (kg/s)

$\dot{m}_Z$ flow rate of species Z in exhaust stack (kg/s)

$\dot{m}_{soot}$ mass flow rate of soot in exhaust stack (kg/s)

$\dot{Q}$ total heat release (kW)

T_o 273 K

T_S exhaust stack temperature (K)

$\dot{V}$ volume flow rate in exhaust stack (m^3/s), at the actual temperature where the photometer is located

X mole fraction (mol/mol)

γ molar C/H ratio, as measured in the cone calorimeter

ρ_{soot} soot density (kg/m^3)

σ_{soot} specific extinction area of soot (12 000 m^2/kg)

superscript A refers to concentrations in the analyser

superscript S refers to concentrations in the exhaust stack

The specimen mass loss rate is computed on the basis of having information about the molecular composition of the fuel pyrolysates and on being able to measure flow rates of certain products of combustion.

The mass loss rate of the specimen is equal to the mass flow rate of the combustion products being generated, minus the mass flow rate of the oxygen being removed:

$$\dot{m} = \dot{m}_{CO_2} + \dot{m}_{CO} + \dot{m}_{H_2O} + \dot{m}_{soot} + \dot{m}_{HCl} + \dot{m}_{HCN} - \left(\dot{m}_{O_2}^o - \dot{m}_{O_2} \right)$$

$$\dot{m} = \Phi \frac{\dot{V}}{22,4}\left(\frac{T_0}{T_S}\right) + \frac{k\dot{V}}{\sigma_{soot}} + f_{HCl}\dot{m} + f_{HCN}\dot{m} - \frac{\dot{Q}}{13\,100}$$

where

$$k = \sigma_{soot}\,\rho_{soot}$$

and

$$\Phi = 44 X_{CO_2}^S + 28 X_{CO}^S + 18 X_{H_2O}^S$$

The concentrations measured in the CO and CO_2 analysers must be corrected to account for the trapping of the water, in order to determine their actual concentrations in the exhaust stack. Hence,

$$\Phi = \left(44 X_{CO_2}^A + 28 X_{CO}^A\right)\left(1 - X_{H_2O}^S\right) + 18 X_{H_2O}^S$$

Since the concentration of H_2O is the exhaust stack, its value will have to be estimated.

A C/H ratio, γ, is defined as the molar ratio of carbon to hydrogen that is going into CO_2, CO, and H_2O; this does not include contributions of C or H which go into HCl or HCN, since the latter are not measured in real scale.

$$\gamma = \frac{X_{CO_2}^S + X_{CO}^S}{2 X_{H_2O}^S} = \left(X_{CO_2}^A + X_{CO}^A\right)\frac{\left(1 - X_{H_2O}^S\right)}{2 X_{H_2O}^S}$$

Solving for $X_{H_2O}^S$

$$X_{H_2O}^S = \frac{\left(X_{CO_2}^A + X_{CO}^A\right)}{2\gamma + X_{CO_2}^A + X_{CO}^A}$$

Since the yields of CO_2, CO and H_2O (i.e., $f_{CO_2}, f_{CO}, f_{H_2O}$) are measured in the cone, the molar ratio γ is expressed in terms of these yields:

$$\gamma = \frac{9}{4}\frac{\left(\frac{1}{11}f_{CO_2} + \frac{1}{7}f_{CO}\right)}{f_{H_2O}}$$

$$\Phi = \left(44 X_{CO_2}^A + 28 X_{CO_2}^A\right)\left(1 - \frac{X_{CO_2}^A + X_{CO}^A}{2\gamma + X_{CO_2}^A + X_{CO}^A}\right) + \frac{18\left(X_{CO_2}^A + X_{CO}^A\right)}{2\gamma + X_{CO_2}^A + X_{CO}^A}$$

$$\Phi = \frac{\left(44 X_{CO_2}^A + 28 X_{CO_2}^A\right)(2\gamma) + 18\left(X_{CO_2}^A + X_{CO}^A\right)}{2\gamma + X_{CO_2}^A + X_{CO}^A}$$

$$\Phi = \frac{(18 + 88\gamma) X_{CO_2} + (18 + 56\gamma) X_{CO}}{2\gamma + X_{CO_2} + X_{CO}}$$

© ISO 2001 – All rights reserved

$$\dot{m} = \frac{\Phi \dfrac{\dot{V}}{22,4}\left(\dfrac{T_0}{T_S}\right) + \dfrac{k\dot{V}}{\sigma_{soot}} - \dfrac{\dot{Q}}{13\,100}}{1 - f_{HCl} - f_{HCN}}$$

Finally giving:

$$\dot{m} = \frac{\dfrac{2\dot{V}}{22,4}\left(\dfrac{T_0}{T_S}\right)\left[\dfrac{(44\gamma + 9)\,X_{CO_2}^{A} + (28\gamma + 9)\,X_{CO}^{A}}{X_{CO_2}^{A} + X_{CO}^{A} + 2\gamma}\right] + \dfrac{k\dot{V}}{\sigma_{soot}} - \dfrac{\dot{Q}}{13\,100}}{1 - f_{HCl} - f_{HCN}}$$

Annex D

Overview of other test protocols using similar equipment

D.1 Pipe insulations

NT FIRE 036 [26] describes a test method to evaluate the contribution to fire growth and smoke production provided by pipe insulations mounted in the ceiling. Heat release and smoke production rates are measured for the early stages of a fire, prior to flash over. The pipe insulations are mounted on metal pipes or bars beneath the ceiling of the ISO 9705 room. The insulation is exposed to flames from the standard ignition source described in ISO 9705 which is placed near the rear wall at a height of 1 m. Its centre is placed 0,5 m from the rear wall and 1,2 m from the side walls. The heat output to the burner during a test is 150 kW over 15 min. During the test, observations such as ignition of the ceiling, start of flame spread, flames emerging out of the doorway, deformation, falling down, melting, burning drops etc. are recorded. A schematic overview of the test set up is given in Figure D.1.
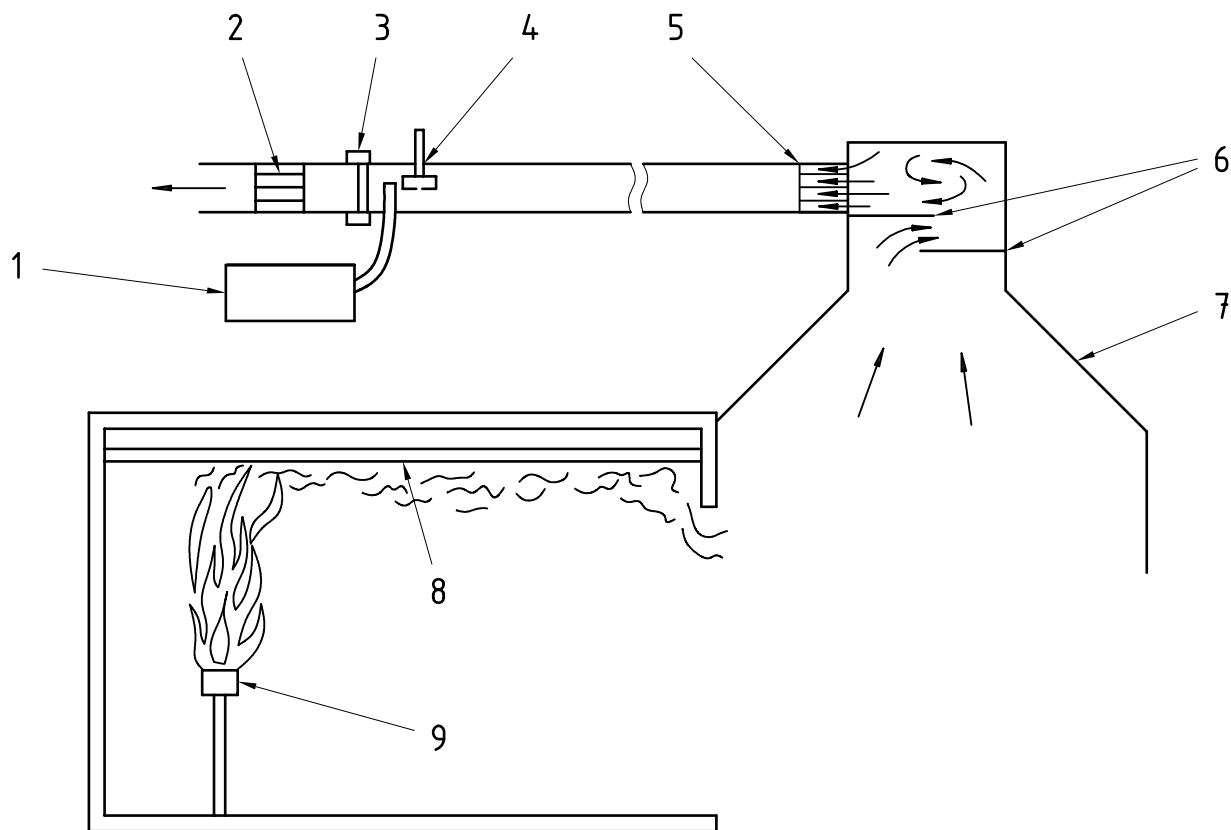
Key

1 Gas analysis

2 Guide vanes

3 Lamp/photo cell system

4 Pitot tube

5 Guide vanes

6 Baffles

7 Hood

8 Pipe insulation

9 Gas burner

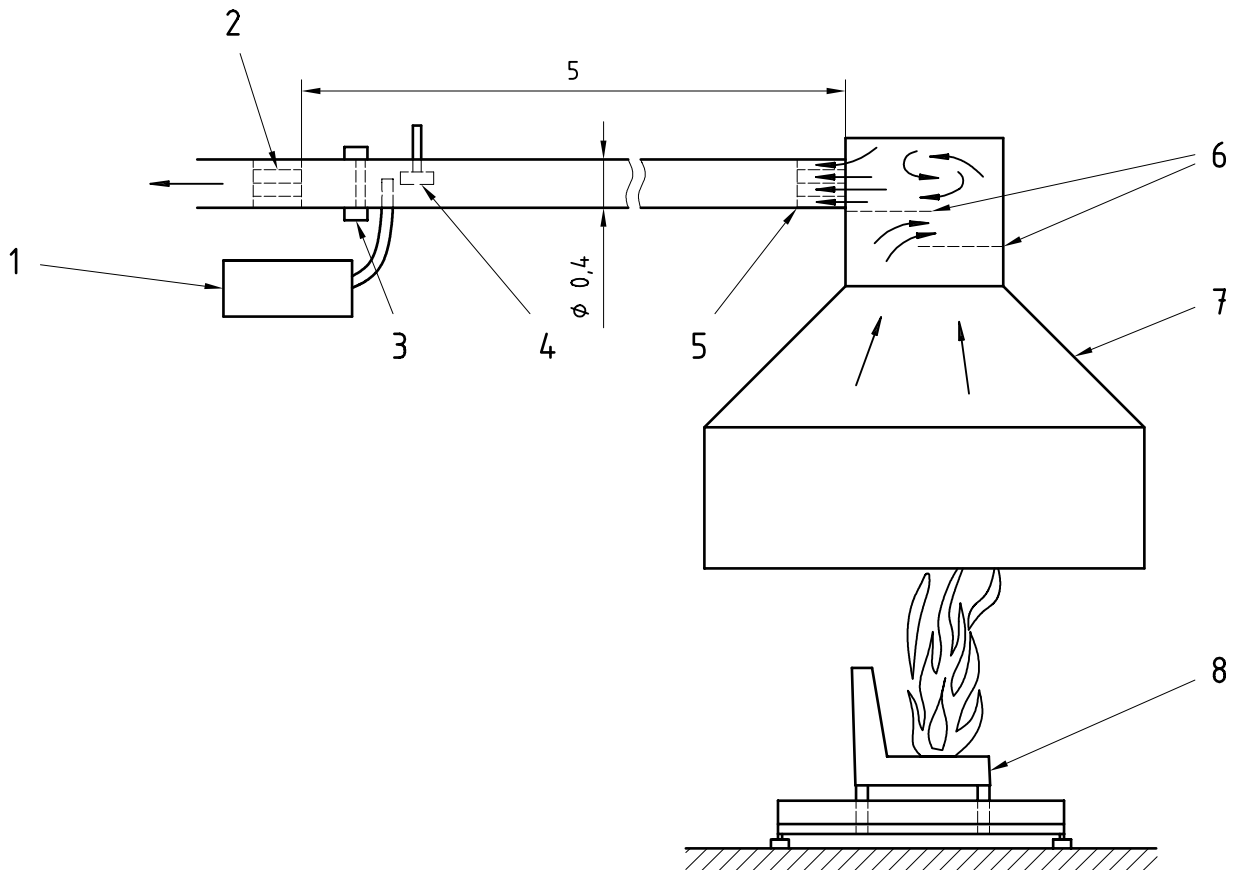**Figure D.1 — Test principle of NT FIRE 036**

D.2 Furniture

Different test protocols exist for furniture. They can be divided into two main groups:

⎯ test protocols where the furniture is positioned inside the ISO 9705 room or a room with other dimensions;

⎯ test protocols where the furniture is positioned under the exhaust hood described in ISO 9705 and which are mostly referred to as furniture calorimeter test protocols or standards.

Depending on the test protocol or the relevant standard, the measurements listed in ISO 9705 can be performed. In most cases an additional weight loss measurement is added by means of a weighing platform. An example of a test set-up for a furniture calorimeter is given in Figure D.2. The ignition source for these tests can vary from standard ignition sources for upholstered furniture such as smouldering cigarettes, gas flames, square ring burners, wooden cribs to specific user defined ignition sources. The most advanced and detailed test protocol developed for both a room test and a furniture calorimeter test is given in the final report of the CBUF project (Combustion Behaviour of Upholstered Furniture).

Dimensions in metres

Key

1	Gas analysis	5	Guide vanes
2	Guide vanes	6	Baffles
3	Lamp/photo cell system	7	Hood $3,0 \times 3,0$
4	Pitot tube	8	Test specimen on weighing platform

Figure D.2 — Test principle of a furniture calorimeter test

D.3 Curtains

In NT FIRE 043 [27] a full-scale test procedure is given for large free hanging curtains with dimensions of 3 100 mm × 3 000 mm. Under the curtain a gas burner similar to the standard ignition source of ISO 9705 is placed. The heat output of this burner is 100 kW for 5 min. The curtains are positioned at about 0,1 m from a wall. A schematic overview of the test set up is given in Figure D.3.
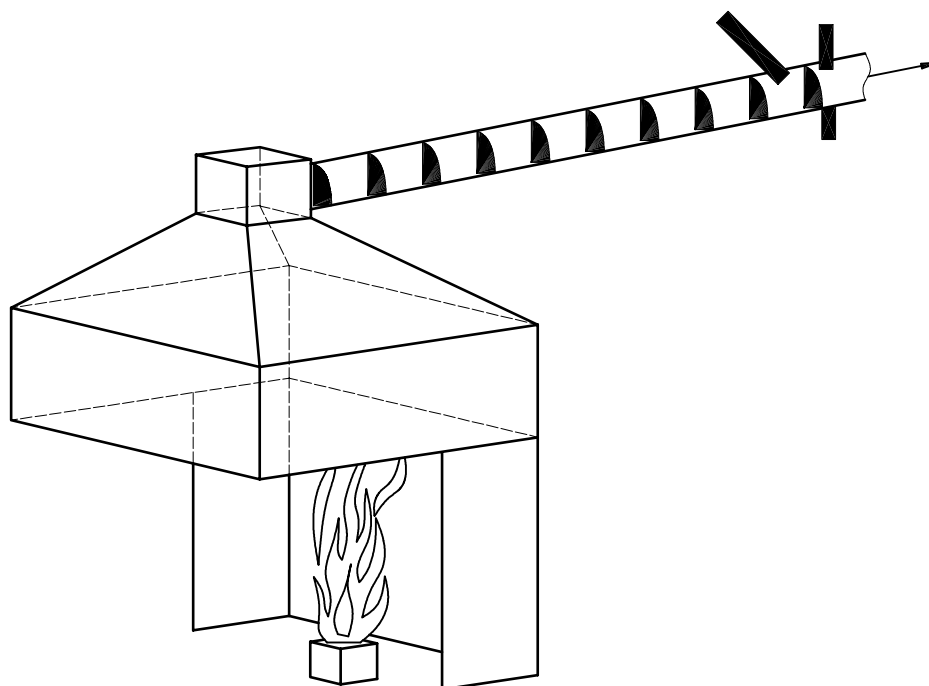
Figure D.3 — Test principle of NT FIRE 043

D.4 Room/corridor

In cases where the burning behaviour of the linings is studied not only in a room but also for instance in a room corridor rig, the same test principle can be used if all combustion gases coming out of the test rig are collected within the ISO 9705 hood. Recently some projects have successfully been applying this technique both for wall and ceiling lining as for floor coverings.

Bibliography

[1] NT FIRE 025, *Surface products — Room fire tests in full scale.* Edition 2, 1991-05, Nordtest.

[2] M. KOKKALA, Sensitivity of the room corner test to variations in the test system and products properties. *Fire and Materials*, **17**, pp. 217-224, 1993.

[3] ASTM E603-98a, *Standard Guide for Room Fire Experiments.*

[4] M. JANSSENS, Modeling the burner source used in the ASTM room fire test, *Journal of Fire Protection Engineering*, **5,** No.2, pp 53-66, 1993.

[5] B. SUNDSTRÖM, *Full scale fire testing of surface materials — Measurements of heat release and productions of smoke and gas species*, SP report 1986-45, SP, 1986.

[6] M. JANSSENS, *Fundamental thermophysical characteristics of wood and their role in enclosure fire growth.* Universiteit Gent, 1991.

[7] Eurefic, *Proceedings of Eurefic Seminar*, Interscience, 1991.

[8] R.WILLIAMSON, N. DEMSBEY, The effect of ignition source exposure and specimen configuration on the fire growth characteristics of a combustible interior finish material, *Fire Safety Journal*, **21,** pp. 313-330, 1993.

[9] U. WICKSTRÖM, B. SUNDSTRÖM, *Fire: Full scale tests: Calibration of the room tests,* Part 1. SP report SP 1981-48, SP 1981.

[10] NFPA, SFPE, *Handbook for Fire Engineering*, NFPA, 1988.

[11] K.STECKLER, H. BAUM, J. QUINTIERE, *Fire induced flows through room openings — Flow coefficients*, 12th Symposium on Combustion, pp. 1591-1600, The Combustion Institute, Pittsburg, 1984.

[12] J. BREESE, R. PEACOCK, *A users guide for RAPID.* Special Publication 722, NBS, 1986.

[13] V. BABRAUSKAS et al. *The role of bench scale test data in assessing real scale fire toxicity*, NIST Technical Note 1284, NIST, 1991.

[14] J.MANGS, E. MIKKOLA, M. KOKKALA, *Room corner test RR*, ISO TC92/SC1/WG7/N84, VTT, Finland, 1990.

[15] J. BEITEL, *ASTM RR report*, ISO TC92/SC1/WG7/N159, 1994.

[16] M.KOKKALA et al., Effects of ignition source in room fire tests, *Fire Science and Technology*, **7**, No.1, 1987.

[17] U. WICKSTRÖM, B. SUNDSTRÖM, *Fire: Full scale tests: Background and test arrangement*, SP report SP 1980-14, SP, 1980.

[18] B. SUNDSTRÖM, Ingrid WETTERLUND, *Fire tests: Building products fire spread and smoke production in full scale*, SP report SP 1985-44, SP, 1985.

[19] B. SUNDSTRÖM, *Room fire test in full scale for surface products.* SP report SP 1984-16, SP, 1984.

[20] U. WICKSTRÖM, U. GÖRANNSON, *Prediction of heat release rates of surface materials in large scale fire test based on cone calorimeter results.*

[21] B. KARLSSON, Models for calculating flame spread on wall lining materials and the resulting heat release rate in the room, *Fire Safety Journal*, **23**, No. 4, 1994.

[22] J. QUINTIERE, *Estimating fire growth on compartment interior finish materials*, ISO TC 92/SC1/WG8/N86.

[23] J. QUINTIERE, B. RHODES, *Fire growth models for materials*. NIST-GCR-94-647, NIST, 1994.

[24] I. WETTERLUND, U. GÖRANSSON, *New method for fire testing of pipe insulation in full scale*, SP report 1986-33, SP, 1986.

[25] NT FIRE 032, *Upholstered furniture full scale test*, Edition 2, Nordtest, 1991-05.

[26] NT FIRE 036, *Pipe insulation, fire spread and smoke production: Full scale test*, Nordtest, 1988-02.

[27] NT FIRE 043, *Large, free hanging curtain and drapery textiles: heat release, fire spread and smoke production — Full scale test*, Nordtest, 1989-09.

[28] B. SUNDSTRÖM, *Fire safety of Upholstered Furniture — The final report*. European Commission Measurement and Testing Report EUR 16477 EN, edited by B. Sundström, Borås, 1995.

[29] P. VAN HEES, *Wind-aided flame spread of floor coverings. Development and validation of large scale and small scale test methods*, University of Gent (in Dutch), 1995.

[30] F. MOWRER, R. WILLIAMSON, *Flame spread evaluation for thin interior finish materials*, Proceedings of the third IAFSS Symposium, pp. 689-698, 1991.

[31] SAITO, K, QUINTIERE, J.G., WILLIAMS, F.A., *Upward Turbulent Flame Spread*, Proceedings First International Symposium on Fire Safety Science, Hemisphere Publishing Corporation, New York, 1984.

[32] THOMAS, P.H., KARLSSON, B., *On Upward Flame Spread On Thick Fuels*, Report LUTVDG/TVBB 3058, Department of Fire Safety Engineering, Lund University, Lund, 1992.

[33] B. KARLSSON, *Modeling fire growth on combustible lining materials in enclosures*, Lund University, Report TVBB-1009, Lund, 1992.

[34] HOSSER, D., DOBBERNACK, R. Und Will, J. *Abschluβberight, Groβmaβstäbliche Raumbrandversuche zur Überprüfung und Absicherung eines sauerstoffkalorimetrischen Prüfverfahrens für Bauprodukte und eines vertikalen Brandausbreitungsmodells*, AZ: RS 11 2 - 67 41 02 – 93 42, Braunschweig, 20.02.1996.

[35] JANSSENS, M. and PARKER, J. *Oxygen Consumption Calorimetry*, pp. 31-59. In *Heat Release in Fires*, Edited by V. Brabauskas and S.J. Grayson. Elsevier Science Publishing, New York, 1992.

[36] BABRAUSKAS, V., HARRIS R. et al, *The Role of Bench-Scale Test Data in Assessing Real-Scale Fire Toxicity*, NIST Technical Note 1284, NIST, 1991.

[37] ISO 5660-1:1993, *Fire tests — Reaction to fire — Part 1: Rate of heat release from building products — (Cone calorimeter method)*.

[38] ISO 5725:1986, *Precision of test methods — Determination of repeatability and reproducibility for a standard test method by inter-laboratory tests*.

[39] ISO 9705:1993, *Fire tests — Full-scale room test for surface products*.

[40] ISO/TR 11696-1:1999, *Uses of reaction to fire test results — Part 1: Application of test results to predict fire performance of internal linings and other building products*.

[41] ISO/TR 11696-2:1999, *Uses of reaction to fire test results — Part 2: Fire hazard assessment of construction products*.

[42] NT FIRE 47, *Combustible products: smoke gas concentrations, continuous FTIR analysis*. Nordtest, 1993-05.

ICS 13.220.50

Price based on 39 pages

© ISO 2001 – All rights reserved